Published in final edited form as:

J Med Chem. 2014 January 23; 57(2): 364–377. doi:10.1021/jm401292m.

Inhibition of 5-oxo-6,8,11,14-eicosatetraenoic acid-induced Activation of Neutrophils and Eosinophils by Novel Indole OXE Receptor Antagonists

Vivek Gore[‡], **Sylvie Gravel**[†], **Chantal Cossette**[†], **Pranav Patel**[‡], **Shishir Chourey**[‡], **Qiuji Ye**[‡], **Joshua Rokach**[‡], **William S. Powell**[†,*]

[†]Meakins-Christie Laboratories, Department of Medicine, McGill University, 3626 St. Urbain Street, Montreal, Quebec H2X 2P2, Canada

[‡]Claude Pepper Institute and Department of Chemistry, Florida Institute of Technology, 150 West University Boulevard, Melbourne, Florida 32901, United States

Abstract

5-Oxo-6,8,11,14-eicosatetraenoic acid (5-oxo-ETE) is a 5-lipoxygenase product that is a potent granulocyte chemoattractant, which induces the infiltration of eosinophils into human skin when injected intradermally. It could therefore be an important proinflammatory mediator in eosinophilic diseases such as asthma and allergic rhinitis and the OXE receptor, which mediates its actions, is therefore an attractive drug target. Using a structure-based approach in which substituents mimicking the essential polar (C_1-C_5) and hydrophobic (C_{15}-C_{20}) regions of 5-oxo-ETE were incorporated on an indole scaffold, we identified two potent selective OXE antagonists with IC_{50} values of about 30 nM. Neither compound displayed agonist activity and both inhibited 5-oxo-ETE-induced chemotaxis and actin polymerization and were relatively resistant to metabolism by rat liver homogenates. The active enantiomers of these racemic antagonists were even more potent, with IC_{50} values of <10 nM. These selective OXE antagonists could potentially be useful therapeutic agents in allergic diseases such as asthma.

Keywords

5-oxo-ETE; 5-lipoxygenase; antagonist; neutrophil; eosinophil; indole; oxovalerate; chemotaxis; actin; asthma; inflammation

INTRODUCTION

The 5-lipoxygenase (5-LO) pathway is responsible for the conversion of arachidonic acid (AA) to a group of potent proinflammatory lipid mediators. 5-LO initially converts AA to

[*]**Corresponding Author** Telephone: 514-398-3864 ext. 094071, Fax: 514-398-7483, William.Powell@McGill.ca.

Present addresses

Vivek Gore, Ph.D., Navinta LLC, 1499 Lower Ferry Road, Ewing, NJ 08618, vivek.gore@navinta.com; Phone: 609-883-1135

Pranav Patel, Ph.D., Navinta LLC, 1499 Lower Ferry Road, Ewing, NJ 08618, pranav.patel@navinta.com; Phone: 609-883-1135

The authors declare no competing financial interest. WSP and JR have applied for US and European patents covering the compounds listed in this paper

5*S*-hydroperoxy-6,8,11,14-eicosatetraenoic acid (5-HpETE) (Figure 1). A portion of the latter intermediate remains bound to 5-LO and is cyclized to the unstable epoxide leukotriene (LT) A_4, the precursor for LTB_4, LTC_4, and LTD_4.[1] However, substantial amounts of 5-HpETE are released from 5-LO and are rapidly reduced by peroxidase to 5*S*-hydroxy-6,8,11,14-eicosatetraenoic acid (5-HETE). 5-HETE is then oxidized to 5-oxo-6,8,11,14-eicosatetraenoic acid (5-oxo-ETE) by 5-hydroxyeicosanoid dehydrogenase (5-HEDH), a highly selective $NADP^+$-dependent enzyme that is widely expressed in both inflammatory and structural cells.[2, 3] 5-Oxo-ETE synthesis is strongly enhanced by activation of the respiratory burst[4] and in the presence of oxidative stress,[5, 6] both of which elevate the levels of the essential cofactor $NADP^+$.

Both LTs[7] and 5-oxo-ETE have potent biological actions that are mediated by G protein-coupled receptors.[8-10] LTB_4, acting through the BLT_1 receptor, is a potent neutrophil chemoattractant, whereas LTD_4 stimulates smooth muscle contraction, vascular leak, mucus secretion, and cytokine release, which are mediated by the $cysLT_1$ and $cysLT_2$ receptors. 5-Oxo-ETE is a potent eosinophil chemoattractant, both *in vitro*[11] and *in vivo*.[12] Its actions are mediated by the OXE receptor,[13-16] which is highly expressed on eosinophils, basophils [17, 18], and neutrophils and, to a lesser extent, on macrophages.[15] 5-Oxo-ETE has also been reported to be an endogenous promoter of the proliferation of tumor cells, which express both the OXE receptor [19] and 5-HEDH.[20]

Metabolism of 5-oxo-ETE by various pathways results in dramatically reduced biological activity.[21] The major metabolic pathway in neutrophils is ω-oxidation by CYP4F3A to 5-oxo-20-hydroxy-ETE, which is 100 times less potent than 5-oxo-ETE. Reduction of 5-oxo-ETE back to 5-HETE by 5-HEDH, which is a reversible enzyme, also reduces potency by 100 times. An even greater 1000-fold reduction in potency occurs after reduction of the 6-*trans* double bond by eicosanoid Δ^6-reductase, a calcium-dependent enzyme also found in neutrophils. A smaller 5-fold reduction in potency is observed after isomerisation of the 8-*cis* double bond to the trans configuration, whereas methylation of the carboxyl group reduces potency by about 20 times.[10, 22] Other oxo-ETEs such as 12-oxo-ETE and 15-oxo-ETE do not activate the OXE receptor. Further extensive structure-activity studies revealed that a fatty acid chain length of at least 18 carbons and a 5-oxo-$\Delta^{6,8}$ diene system are the minimum requirements for activation of this receptor.[23]

The potent chemoattractant effects of 5-oxo-ETE on eosinophils suggest that it may play an important role in eosinophilic diseases such as asthma and allergic rhinitis. However, progress in understanding its pathophysiological role has been impeded by the lack of an ortholog of the OXE receptor in rodents. An alternative approach to investigate its biological role would be the use of selective antagonists. To date, little information is available about such compounds. We previously showed that 5-oxo-12-HETE, a metabolite of 5-oxo-ETE formed by platelets, while not itself affecting intracellular calcium levels in neutrophils, blocks 5-oxo-ETE-induced calcium mobilization with an IC_{50} of 0.5μM.[24] However, this substance is not very stable and is not suitable for development as an antagonist. Another very recent report documented antagonist properties for the benzobisthiazole derivative, Gue1654.[25] The goal of the present study was to develop an OXE receptor antagonist using an indole scaffold containing substituents mimicking both the polar 5-oxovalerate portion of

5-oxo-ETE as well as the hydrophobic ω-end of the molecule (Figure 2A). In an initial study we recently reported antagonist activity in the μmolar range of N-acyl-2-hexyl indoles.[26] We have now developed a much more potent compound in this series and have identified a second series of indoles with comparable OXE receptor antagonist potency.

RESULTS

OXE receptor antagonist effects of indoles containing hexyl and 5-oxovalerate substituents

Our initial strategy was to examine the effects of a series of indoles containing two substituents: a 5-oxo-valeryl group and a hexyl group to mimic the carboxyl and alkyl portions, respectively, of 5-oxo-ETE. Addition of 5-oxo-ETE (10 nM) to indo-1-loaded neutrophils resulted in a strong calcium response (Figure 2B). Panels C to G of Figure 2 show the effects of a series of N-(5-oxovaleryl) indoles (10 μM) containing hexyl substituents in different positions.

As we previously reported,[26] 5-oxo-ETE-induced calcium mobilization was completely abolished by the indole containing a hexyl group in the 2-position (**10**, Figure 2C), but was hardly affected when the hexyl group was present in the 3-, 5-, or 6-positions (Figure 2 D-G) and was only modestly effected when the hexyl group was in the 7-position (Figure 2G). In addition to the N-acyl indoles described above we now also prepared two indoles containing a 5-oxovaleryl substituent in the 3-position. The presence of a 2-hexyl group in this series inhibited calcium mobilization by about 50% (Figure 2I), whereas a 1-hexyl substituent had a smaller effect (Figure 2H). The synthesis of derivatives in panel B to G has been reported by us previously.[23] The compounds in panels H and I, and their bioactivity have not been reported previously.

Effects of modification of the alkyl group on the antagonist potency of 1-acylindoles

We initially focused on the most potent antagonist, **10**, and examined the effects of various modifications of the alkyl side chain (Figure 3). Reduction of its length to 5 carbons (**9**) resulted in a small decrease in potency, whereas further shortening to a butyl group (**8**) had a much more dramatic effect, reducing the potency by over 10-fold. In contrast, increasing the length of the side chain to seven (**11**), eight (**12**), or eleven (**13**) carbons appeared to result in slightly increased potency. These compounds were synthesized from the common precursor 1H-indole-2-carboxylic acid as shown in Scheme 1 and the detailed synthesis is reported previously.[23] Introduction of a single double bond in conjugation with the aromatic system reduced potency in the 6-carbon series (Δ^1Hx (**14**) vs Hx (**10**)), but had little effect in the 11-carbon series (Δ^1Un (**15**) vs Un (**13**)). The compounds shown in Figure 2 were synthesized as shown in Schemes 2 and 3.

Effects of modification of the 5-oxovalerate group of 1-acyl-2-hexylindoles

We next investigated the effects of various structural modifications of the carboxyl side chain in a series of N-acyl-2-hexyl indoles (Figure 4). Shortening the side chain to 4 carbons (**29**; 4-oxobutyrate) nearly eliminated antagonist activity. Addition of two methyl groups to the 3-position of 5-oxovalerate (**17**) reduced potency by about 10-fold, whereas placing a

cyclopropyl group (**25**) in this position had relatively little effect. In contrast, addition of a single methyl group to the 3-position (**27**) increased potency by over 10 times, resulting in an IC_{50} of 90 nM. The structural modifications shown in Figure 4 were performed as described in Schemes 3-6.

Effects of halides and other substituents on the potency of 1-acyl-2-hexylindoles

Focusing on compound **27**, we investigated the effects of additional substituents on the indole moiety. The presence of a methyl group in the 3-position (**47**) or a chloro substituent in the 5-position (**41**) had relatively little effect on antagonist potency. On the other hand, a 5-bromo substituent (**42**) or a 6-methoxy group (**36**) reduced potency by several fold. In contrast, addition of either a chloro (**34**) or a bromo (**35**) substituent at the 6-position resulted in increases in potency of approximately 3-fold. The 6-chloroindole **34** is a potent OXE receptor antagonist with an IC_{50} value of 28 nM. These aromatic substituted compounds were synthesized as shown in Schemes 7-9.

Antagonist effects of a second series of indoles

Because of the modest antagonist effect of 2-hexyl-3-(5-oxo-valerate)indole (**48**) as illustrated by Figure 2I we decided to test the effects of various modifications of this compound. Since methylation of the indole nitrogen (**50**; Figure 6) slightly increased potency, an N-methyl group was incorporated in all further compounds in this series, the syntheses of which are shown in Schemes 10-13. We focused primarily on the effects of modifications analogous to those employed in the 1-acylindole series. Addition of a chloro substituent in the 5-position of the indole ring (**51**; IC_{50}, 566 nM) increased potency by about 10 times, whereas addition of a methyl group at the 3-position of the 5-oxovalerate side chain (**52**; IC_{50}, 314 nM) had a slightly greater effect. Combination of these two modifications (compound **53**, IC_{50}, 28 nM) resulted in a further increase in potency of over 10-fold. In contrast to the 1-acyl series, the 5-chloro compound **53** was considerably more potent than the 6-chloro derivative **56**. The corresponding 5-bromo derivative **54** was equipotent with **53**. The acyl side chain was substituted at C_3 on the indole ring as shown in Scheme 10. Further modifications were performed as shown in Schemes 11 to 13.

Compounds 53 and 34 are selective OXE receptor antagonists

The selectivities of the two most potent compounds (**53** and **34**) were further investigated (Figure 7). Following addition of vehicle to neutrophils, 5-oxo-ETE elicited a robust calcium response that did not affect the responses to subsequent addition of LTB_4, PAF, fMLP, or IL-8 (bottom tracings in Figure 7, panels A, B, C and D, respectively). Prior addition of high concentrations (10 μM) of **53** (middle tracings) and **34** (upper tracings) completely blocked 5-oxo-ETE-induced calcium mobilization but had no effect on the responses to any of the other four agonists shown in Figure 7, indicating that these antagonists are highly selective for the OXE receptor.

Compounds 53 and 34 block 5-oxo-ETE-induced actin polymerization and chemotaxis

The effects of **53** and **34** on 5-oxo-ETE-induced actin polymerization in both eosinophils and neutrophils were investigated using flow cytometry. Leukocytes were preincubated with

either vehicle, **53**, or **34** for 5 min followed by incubation with 5-oxo-ETE (10 nM) for a further 20 s and the amounts of polymerized F-actin were determined in both eosinophils and neutrophils. Both **53** (IC_{50},33 ± 10 nM) and **34** (IC_{50}, 30 ± 7 nM) were potent inhibitors of 5-oxo-ETE-induced actin polymerization in eosinophils (Figure 8A) and had similar effects on neutrophils (Figure 8B). **53** (IC_{50}, 454 ±192 nM) and **34** (IC_{50}, 402 ± 120 nM) also inhibited 5-oxo-ETE induced neutrophil chemotaxis (Figure 8C). The IC_{50} values were higher in this assay because we used a higher concentration of 5-oxo-ETE (100 nM) to induce neutrophil migration.

The benzobisthiazole derivative Gue1654 was recently reported to block Gβγ- but not $G\alpha_i$-mediated responses to 5-oxo-ETE.[25] We found that this compound is about 10 times less potent than **53** and **34** in blocking 5-oxo-ETE-induced actin polymerization in eosinophils (Figure 8A) and neutrophils (Figure 8B).

Metabolism of 34 and 53 by rat liver homogenates

To determine whether **53** and **34** are susceptible to metabolism, they were incubated with rat liver homogenates. Negligible metabolism of either compound was observed in medium that favored β-oxidation (containing ATP, CoA, L-carnitine and NAD^+ [27]; data not shown). Compound **34** was metabolized to a small extent when incubated for 60 min with a liver homogenate containing NADPH (1 mM), the cofactor required by cytochrome P450 (Figure 9A). Only one significant product was observed, which had a t_R of 18.2 min, compared to 30.2 min for unmetabolized **34**. The UV spectrum of this product was virtually identical to that of **34** (inset to Figure 9A). **53** was metabolized to an even lesser extent by liver homogenates under identical conditions (Figure 9B). A very small amount of a more polar product (t_R, 14.1 min) was detected, with a UV spectrum nearly identical to that of **53** (inset to Figure 9B).

Antagonist potencies of purified enantiomers of 34 and 53

Because of the presence of a methyl group in the 3-position of the 5-oxo-valerate substituents of **34** and **53**, both compounds are racemic mixtures. To determine whether the individual enantiomers of each pair differed from one another in their antagonist potencies, they were separated by chiral HPLC. The enantiomers of **34** were completely resolved in a single chromatography to give two peaks, designated as **34a** and **34b** (Figure 10A). It was not possible to completely separate the two enantiomers of **53** (designated as **53a** and **53b**) in a single chromatography (Figure 10D) and a second step of HPLC using the same conditions was required to purify **53b**. Chiral HPLC of the purified enantiomers is shown in Figure 10, panels B, C, E and F).

The effects of the above enantiomers on 5-oxo-ETE-induced calcium mobilization in neutrophils was investigated. The purities of the four enantiomers after purification were: **34a** (99.2%), **34b** (99.9%), **53a** (98.8%) and **53b** (98.7%). In both cases the earlier-eluting enantiomers were by far the more potent. **34a** and **53a** had nearly identical IC_{50} values of 7 ± 2 and 6 ± 1 nM, respectively, whereas the later-eluting enantiomers **34b** and **53b** had IC_{50} values of 2175 ± 357 nM and 2730 ± 956 nM, respectively.

DISCUSSION

Because of the potent chemoattractant effect of 5-oxo-ETE on eosinophils and its possible involvement in asthma and other allergic diseases we set out to design a selective antagonist of the OXE receptor that mediates its biological activity. We used a structure-based approach in which we incorporated segments of the 5-oxo-ETE molecule that are essential for its biological activity onto an indole backbone. We previously identified several regions of 5-oxo-ETE that are critical for leukocyte activation: the C_1 carboxyl group, the 5-oxo-$\Delta^{6,8}$-diene system, and the terminal hydrophobic ω-end of the molecule.[23] Based on this information we designed a series of indole derivatives containing both the C_1-C_5 portion of 5-oxo-ETE (i.e. a 5-oxovalerate group) and the C_{15}-C_{20} portion of the molecule in the form of a hexyl group. Since the oxo group in these compounds is conjugated with the aromatic indole system, the indole moiety should mimic the conjugated diene portion of 5-oxo-ETE as well as fix the positions of the alkyl and acyl side chains relative to one another. Different positional isomers can thereby mimic various conformational forms of 5-oxo-ETE that may bind to and subsequently activate the OXE receptor. An ideal OXE receptor antagonist would possess a structure that mimicked the conformation of 5-oxo-ETE that has high affinity for the receptor, but could not alter its conformation to mimic the one that serves to initiate OXE receptor signaling via G-proteins.

We identified two series of indoles with potent antagonist activities containing a 5-oxovalerate moiety in either the 1-position or the 3-position. Our preliminary studies revealed that a hydrophobic side chain is required for activity, as 1(5-oxovalerate)indole had no detectable activity at a concentration of 30 μM.[26] The present results clearly indicate that the alkyl group must be adjacent to the acyl side chain in both of the above series, since further separation of the two side chains resulted in dramatic losses in antagonist potency. This suggests that both series can mimic a hairpin conformation of 5-oxo-ETE that can bind to the OXE receptor without activating it. The indole structure itself also appears to play a role, as we synthesized an analogous quinoline derivative with a hexyl group in the 2-position and 5-oxovalerate in the 3-position. Although this compound did not act as an agonist, it had only very weak antagonist activity, with an IC_{50} above 30 μM (data not shown), suggesting that the angle between the two side chains may be important (5- vs 6-membered ring).

We tested several modifications of the alkyl side chain. Whereas reducing its length to 4 or 5 carbons reduced potency, increasing the length to seven, eight, or eleven carbons appeared to slightly increase potency. However, lengthening this side chain also reduced solubility and, in the cases of high concentrations (30 μM) of the C_8 and C_{11} compounds, resulted in some calcium mobilization, which was not observed in compounds containing a hexyl substituent. Although carbon-15 of 5-oxo-ETE is part of an olefinic group, it seemed unlikely that an unsaturated carbon in the hexyl group would be required, as saturation of the Δ^{14}-double bond of 5-oxo-ETE (as in 5-oxo-6,8,11-eicosatrienoic acid) did not reduce biological potency.[23] Nevertheless, we also investigated the effects of replacing the hexyl group with a Δ^{1}-hexenyl group, but found that this reduced antagonist potency. However, this was not true with a C_{11} side chain, in which case there was little difference in the potencies of

undecyl and Δ^1-undecenyl derivatives. For the above reasons we focused on 2-hexylindoles in subsequent studies.

We also investigated the effects of modification of the 5-oxovalerate substituent, in part as an attempt to block any potential metabolism by β-oxidation. Addition of bulky groups (dimethyl or cyclopropyl) to the 3-position of the 5-oxovalerate moiety either reduced potency or had little effect. In contrast, addition of a single methyl group to this position dramatically increased potency in both the 1-acyl and 3-acyl series. The 3-methyl group presumably favors a conformation of the acyl side chain that interacts strongly with the OXE receptor, resulting in increased potency. This modification would also have the additional advantage of blocking β-oxidation, and we found no evidence for the metabolism of either **53** or **34** when they were incubated with rat liver homogenates under conditions [27] known to favor this pathway (data not shown).

We previously showed that addition of a chloro group to the 6-position of **10** in the 1-acyl series increases potency by 3-4 fold (IC_{50} of 6-Cl derivative ~0.4 μM), whereas addition of a 5-chloro substituent has no effect.[26] A similar increase in potency was observed in the present study following the addition of a 6-Cl substituent (**34**) to the 1-(3-methyl-5-oxo-valerate) compound **27**, in contrast to the corresponding 5-Cl derivative (**51**) which was, if anything, less potent than **27**. Addition of a 6-Cl substituent also increased potency by about 4-fold in the 3-acyl series (**56** compared to **52** in Figure 6). However, in this case, the corresponding 5-Cl compound (**53**) was even more potent. This may be because the relative positions of the three substituents (3-methyl-5-oxovalerate, hexyl, and Cl) to one another is more important than their absolute positions on the indole ring. If the indole in **53** is inverted as shown in Figure 10, it can be seen that a chloro substituent in the 5-position should mimic the 6-chloro group of **34**. For this reason we wondered whether the presence of a 3-methyl group in the 1-acyl series might increase potency, but this was not the case (compare **27** and **47**, Figure 5). In both the 1-acyl and 3-acyl series Cl could be replaced by Br without affecting potency.

The progression in the SAR from 1(5-oxovalerate)indole and **10**[26] to the novel compounds **27** and **34**, accompanied by their IC_{50} values is shown in Figure 10. A similar progression from the novel 2,3-substituted indole **48** to the highly potent **53** is also shown. Because of their similarity it would seem likely that both **53** and **34** interact similarly with the OXE receptor. However, these two compounds could differ in their rates of absorption or metabolism due to structural differences such as the presence or absence of an amide bond, which could potentially affect their *in vivo* potencies.

Both **34** and **53** were resistant to metabolism by β-oxidation by liver homogenates, whereas **34** was metabolized to a small extent when incubated under conditions favoring metabolism by cytochrome P450, in which case about 12% was converted to a single more polar product. Since the UV spectrum of this compound was identical to that of **34**, it is unlikely that it was formed by alteration or addition to the indole structure. It would seem probable that it is an ω, ω-1, or ω-2 oxidation products formed by hydroxylation of the hexyl group by cytochrome P450. Work on the characterization of this metabolite is currently underway. **53** appeared to be metabolized to a very small extent (~2%) by this pathway. Preliminary

pharmacokinetic experiments in rats suggest that both antagonists appear rapidly in the blood following oral administration, along with smaller amounts of polar metabolites similar to those formed by liver homogenates in the presence of NADPH (unpublished data).

Because both **34** and **53** contain a methyl group in the 3-position of their 5-oxovalerate substituent they are racemates. Separation of the enantiomers by chiral chromatography revealed that in each case a single enantiomer was responsible for the majority of antagonist activity, with the more active enantiomer being several hundred times more potent than the less active one. The preparation of **53b** that we used contained about 1.3% of the more active enantiomer **53a**, which would have contributed to the antagonist effect we observed. Therefore, the true IC_{50} value of **53b** is likely to be even higher than the value of ~2.7 μM that we observed. This was not true for the inactive enantiomer of **34** (i.e. **34b**), which did not contain any detectable amount of **34a**.

Other than our preliminary study {Gore, 2013 2588 /id}, very little information is available on compounds with OXE receptor antagonist activity. We previously found that platelets convert 5-oxo-ETE to metabolites that can block 5-oxo-ETE-induced calcium mobilization in neutrophils.[24] We identified these compounds as the 8-*cis* and 8-*trans* isomers of 5-oxo-12*S*-hydroxy-6,8,10,14-eicosatetraenoic acid (i.e. 5-oxo-12-HETE and 8-*trans*-5-oxo-12-HETE). They were also formed by transcellular biosynthesis in coincubations of platelets with neutrophils. Neither compound mobilized intracellular calcium in neutrophils, but both inhibited 5-oxo-ETE-induced calcium mobilization with IC_{50} values of 0.5 μM (5-oxo-12-HETE) and 2.5 μM (8-*trans*-5-oxo-12-HETE). Although these metabolites would not be good drug candidates because of their instability and susceptibility to metabolism, these findings encouraged us to search for more suitable OXE receptor antagonists.

Long-chain polyunsaturated fatty acids, including 4,7,10,13,16,19-docosahexanenoic acid, 5,8,11,14,17-eicosapentaenoic acid, 8,11,14-eicosatrienoic acid, and 11,14,17-eicosatrienoic acid have been reported to antagonize the stimulatory effects of 5-oxo-ETE on $GTP_{\gamma}S$ binding to an OXE receptor-$G_{\alpha i}$ fusion protein.[14] The IC_{50} values for their inhibitory effects ranged between 2 and 6 μM. Although these results are interesting, these substances would not be of practical use as OXE receptor antagonists because they have various other effects, including, in some cases, activation of inflammatory cells.[28] Furthermore, ω3-polyunsaturated fatty acids can be converted to anti-inflammatory resolvins and protectins that have a variety of independent effects of their own.[29]

It was recently reported that the synthetic compound Gue1654 selectively blocks 5-oxo-ETE-induced calcium mobilization, shape change, and chemotaxis in neutrophils and eosinophils.[30] This compound was identified as a result of screening a selective library using a calcium mobilization assay, followed by virtual screening using a model of the OXE receptor. Although Gue1654 blocked all of the above responses, it failed to prevent the inhibitory effect of 5-oxo-ETE on adenylyl cyclase in neutrophils, indicating that it is a biased ligand for this receptor. In the present study we found that Gue1654 is about one-tenth as potent as **53** and **34** in inhibiting 5-oxo-ETE-induced actin polymerization in neutrophils and eosinophils.

CONCLUSIONS

5-Oxo-ETE is a potent chemoattractant for eosinophils, both *in vitro* [11] and *in vivo* [12] and can also enhance the survival of these cells by stimulating the release of GM-CSF from monocytes.[31] Because of these effects, 5-oxo-ETE may be an important mediator in eosinophilic disorders such as asthma and allergic rhinitis, and selective OXE receptor antagonists such as **53** and **34** may be useful therapeutic agents in these diseases. Both compounds are highly potent, with IC_{50} values of about 30 nM in inhibiting 5-oxo-ETE-induced calcium mobilization and actin polymerization, and are relatively resistant to metabolism by rat liver homogenates. They are both racemic mixtures, and their potencies can be further enhanced by the use of the pure active enantiomers, which have IC_{50} values below 10 nM. It will be very interesting to determine whether these antagonists are effective in disease models in animals possessing the OXE receptor.

EXPERIMENTAL SECTION

Preparation of leukocytes

Whole blood from healthy subjects was mixed with a solution of dextran 500 (from Leuconostoc; Sigma-Aldrich) and the red cells were allowed to sediment under unit gravity at 4 °C for 45 min. The supernatant was centrifuged to give a pellet containing unfractionated leukocytes. The cells in the pellet were subjected to hypotonic lysis and then used to investigate the effects of OXE receptor antagonists on 5-oxo-ETE-indued actin polymerization. Alternatively, for experiments designed to measure intracellular calcium mobilization and chemotaxis in neutrophils, the pellet was resuspended in PBS and centrifuged over Ficoll [32], followed by hypotonic lysis of any remaining red cells. In both cases, the cells were resuspended in PBS (without calcium or magnesium).

Measurement of intracellular calcium levels in neutrophils

Neutrophils were loaded with indo-1 acetoxymethyl ester (Invitrogen, Carlsbad, CA) as described previously.[10] The cells were then washed and resuspended in PBS. Five minutes before commencing data acquisition, the cells were placed in a cuvette and Ca^{++} and Mg^{++} were added to give final concentrations of 1.8 and 1 mM, respectively. The cuvette was then placed in a Deltascan 4000 spectrofluorometer (Photon Technology International, Birmingham, NJ) in a cuvette holder maintained at 37 °C and equipped with a magnetic stirrer. Fluorescence was monitored at excitation and emission wavelengths of 331 and 410 nm, respectively, and the baseline allowed to stabilize before addition of either vehicle (10 μl DMSO) or potential OXE receptor antagonist. Two min later, 5-oxo-ETE (final concentration 10 nM in PBS containing 0.1% BSA) was added, followed 1 min later by addition of digitonin (final concentration, 0.1%) to permit measurement of maximal fluorescence. In some cases a second agonist (LTB_4, PAF, fMLP, or IL-8) was added 2 min after addition of 5-oxo-ETE, followed 1 min later by digitonin. Calcium levels were calculated as previously described.[10]

Evaluation of actin polymerization in neutrophils and eosinophils

F-actin was measured in unfractionated leukocytes prepared as described above. The leukocytes were first incubated for 30 min on ice with allophycocyanin-labeled anti-CD49d (BioLegend, San Diego, CA). After washing with PBS, the cells were suspended in PBS containing Ca^{++} (1.8 mM) and Mg^{++} (1 mM) at a concentration of 5.5×10^6 cells/ml. Aliquots (100 μl) of the fluorescently labelled cells were then preincubated for 5 min at 37 °C with vehicle (1 μl DMSO) or different concentrations of **53**, **34**, or Gue1654, followed by addition of either vehicle (10 μl PBS containing Ca^{++}, Mg^{++}, and 0.1% BSA) or 5-oxo-ETE (final concentration, 10 nM). After 20 s, the incubations were terminated by addition of formaldehyde (37%) to give a final concentration of 8.5%, and kept on ice for 30 min. A mixture of lysophosphatidylcholine (30 μg in 23.8 μl PBS) and N-(7-nitrobenz-2-oxa-1,3-diazol-4-yl)phallacidin (NBD-phallacidin; Molecular Probes; 49 pmol in 6.2 μl methanol; final concentration, 0.3 μM) was added to each sample [33], followed by incubation overnight in the dark at 4 °C. Immediately prior to data acquisition by flow cytometry (FACSCalibur, BD Biosciences, San Jose, CA), 200μl PBS containing 1% formaldehyde was added to each sample. Eosinophils were identified by high side scatter and high expression of CD49d, whereas neutrophils displayed high side scatter but low CD49d expression.

Evaluation of neutrophil migration

Neutrophil migration was measured using a modified Boyden chamber technique with 48-well microchemotaxis chambers (Neuro Probe Inc., Cabin John, MD) and Sartorius cellulose nitrate filters (8 μm pore size; 140 μm thickness; Neuro Probe Inc.).[10] Vehicle (PBS containing Ca^{++}, Mg^{++} and 0.3% BSA) or 5-oxo-ETE (100 ng) were added to the bottom wells, whereas neutrophils (150,000 cells in PBS containing Ca^{++}, Mg^{++} and 0.4% OVA) were added to each of the top wells. Both top and bottom wells also contained either vehicle or different concentrations of **53** or **34**. The chambers were incubated for 2 h at 37 °C in 5% CO, and humidified air. The cells were then stained using hematoxylin (Canada Wide Scientific) followed by chromotrope 2R (Sigma Chemical Co) and the numbers of cells on the bottom surfaces were counted in five different fields at a magnification of 400× for each well. All incubations were performed in triplicate.

Metabolism of 34 and 53 by rat liver homogenates

Liver from male Sprague-Dawley rats was minced in ice-cold 0.25 M sucrose (4 ml/g tissue) and homogenized using 8 strokes in a Potter-Elvehjem homogenizer in an ice bath, followed by centrifugation at 600 × g for 10 min. 0.2 Milliliters of phosphate buffer (pH 7.4, final concentration 50 mM) containing NADPH (final concentration 1 mM) was added to 0.8 ml of the supernatant (referred to as the homogenate) and the mixture was incubated with either **34** or **53** (20 μM) for 60 min at 37 °C. The incubations were terminated by the addition of ice-cold MeOH (0.67 ml) followed by cooling on ice. The products were analyzed by precolumn extraction combined with reversed-phase-HPLC [34] using a modified Waters 2695 Alliance system (Waters Corp., Mississauga, ON) with a photodiode array detector (Waters model 2996). The stationary phase was a Nova-Pak C18 column (150 × 3.9 mm; Waters Corp). The mobile phase was a gradient between 22% and 42% acetonitrile in water with acetic acid (0.02%) and a flow rate of 1 ml/min.

Purification of enantiomers of 34 and 53

34 was separated into its two enantiomer **34a** and **34b** by chiral HPLC using the Waters 2695 Alliance system described above, except that the sample was injected directly into a loop in a 6-port valve. The stationary phase was a Lux Amylose-2 column (250 × 4.6 mm; 3 μm particle size; Phenomenex, Torrance, CA). The mobile phase was hexane/methanol/acetic acid (99:1:0.1) at a flow rate of 1.5 ml/min. The two enantiomers of **53** were purified as described above except that the stationary phase was a Lux Cellulose-1 column (250 × 4.6 mm; 5 μm particle size; Phenomenex, Torrance, CA) and the mobile phase was hexane/methanol/acetic acid (98.5:1.5:0.1). Because the later eluting peak (**53b**) was initially contaminated with about 4% of **53a** it was further purified by a second step of chiral HPLC using identical conditions.

Reagents and methods

Platelet-activating factor (PAF; β-acetyl-γ-O-hexadecyl-L-α-phosphatidylcholine), formyl-met-leu-phe (fMLP), and Gue1654 (7-(methylthio)-2-[(2,2-diphenylacetyl)amino]benzo[1,2-d:4,3-d′]bisthiazole) were obtained from Sigma-Aldrich, whereas interkleukin-8 (IL-8) was purchased from R&D Systems. 5-Oxo-ETE[35] and LTB_4[36] were prepared by chemical synthesis as previously described. All reactions were carried out using dry solvents under argon atmosphere. High-resolution mass spectra were recorded on an AccuTOF mass spectrometer by positive ion ESI mode with DART as an ion source. ^{1}H NMR and ^{13}C NMR spectra were recorded in $CDCl_3$ using TMS as an internal standard on a BRUKER AMX 400 MHz spectrometer at rt. All compounds were analyzed by TLC, HRMS and NMR. Prior to biological assay, the purity of all final compounds was determined to be >95% by NMR and HPLC. HPLC conditions: Waters 2695 Alliance System with Waters Novapak C18 (150 × 3.9 mm) column and photodiode array detector (Waters Model 2996), gradient mobile phase between H_2O/MeCN/MeOH (56:22:22) to H_2O/MeCN/MeOH (16:42:42) over 30 min, both solvents contained 0.02% acetic acid, and a flow rate was 1 mL/min.

Synthesis of 8, 9, 10, 11, 12, 13

These compounds were synthesized from 1H-Indole-2-carboxylic acid (**1**) as described previously.[23]

Synthesis of 5-(2-Hex-1-enyl-indol-1-yl)-5-oxo-pentanoic acid (14)

To a stirred solution of '**5**, n = 3' (15 mg, 0.0753 mmol) in DMSO (0.7 ml) was added KOH (17 mg, 0.301 mmol) at rt and stirred for 1 h. Dihydro-2H-pyran-2,6(3H)-dione (**7**) (34 mg, 0.301 mmol) in DMSO (0.5 ml) was added to the reaction mixture and stirred for 2 h. The mixture was quenched with saturated NH_4Cl, extracted in EtOAc, dried over Na_2SO_4 and purified using column chromatography using 50% EtOAc/Hex as eluent to afford **14** (13 mg, 55%). HRMS (ESI) *m/z* cald for $[C_{19}H_{23}NO_3 + H]^+$: 314.1751, found 314.1763. ^{1}H NMR (400 MHz, $CDCl_3$): δ 8.29 (d, *J* = 8.6 Hz, 1H), 7.41 (dd, *J* = 8.3, 2.5 Hz, 2H), 7.29 (dd, *J* = 8.6, 1.6 Hz, 1H), 7.19 (s, 1H), 6.52 (d, *J* = 3.7 Hz, 1H), 6.38 (d, *J* = 15.8 Hz, 1H), 6.16 (dt, *J* = 15.7, 6.9 Hz, 1H), 3.08-2.59 (m, 3H), 2.43 (ddd, *J* = 47.5, 15.9, 6.5 Hz, 2H), 2.15 (d, *J* = 6.6 Hz, 2H), 1.42-1.27 (m, 4H), 0.86 (t, *J* = 7.2 Hz, 3H). ^{13}C NMR ($CDCl_3$): δ 177.32,

169.95, 133.94, 130.75, 130.51, 129.76, 124.98, 123.31, 118.06, 116.57, 109.39, 41.84, 40.33, 32.74, 31.62, 27.07, 22.28, 20.00, 13.94.

Synthesis of (Z)-5-oxo-5-(2-(undec-1-en-1-yl)-1*H*-indol-1-yl)pentanoic acid (15)

To a solution of '**5**, n = 8' (50 mg, 0.19 mmol) in DMSO (1 ml) was added KOH (42 mg, 0.74mmol) at rt. The reaction mixture was stirred for 30 min followed by the addition of **7** (85 mg, 0.74 mmol). After 3 h the reaction was quenched by adding saturated NH_4Cl solution. The organic layer was extracted with EtOAc, the combined organic layers were washed with brine and dried over Na_2SO_4. The solvents were evaporated under reduced pressure and the crude was purified by silica gel chromatography using 50% EtOAc/Hex as eluent to afford **15** (37.4 mg, 52%). HRMS (ESI) *m/z* cald for $[C_{24}H_{33}NO_3 + H]^+$: 384.2533, found 384.2485. ^{1}H NMR (400 MHz, $CDCl_3$): δ 8.27 (d, *J* = 8.2 Hz, 1H), 7.51 (d, *J* = 7.6 Hz, 1H), 7.34-7.17 (m, 2H), 6.46 (d, *J* = 13.7 Hz, 1H), 5.93-5.82 (m, 1H), 3.03 (t, *J* = 7.0 Hz, 2H), 2.51 (t, *J* = 7.1 Hz, 2H), 2.34 (q, *J* = 7.0 Hz, 2H), 2.12 (p, *J* = 7.0 Hz, 2H), 1.25 (s, 14H), 0.86 (d, *J* = 6.8 Hz, 3H). ^{13}C NMR ($CDCl_3$): δ 177.04, 172.99, 136.76, 135.84, 135.25, 129.40, 124.77, 123.52, 121.10, 120.25, 116.19, 111.44, 37.73, 32.71, 31.89, 29.57, 29.49, 29.43, 29.32, 29.06, 22.68, 20.08, 14.11.

Synthesis of 5-(2-hexyl-1*H*-indol-1-yl)-3,3-dimethyl-5-oxopentanoic acid (17)

To a solution of '**6**, n = 3' (12 mg, 0.06 mmol) in DMSO (0.2 ml) was added KOH (13 mg, 0.24 mmol) at rt. The reaction mixture was then stirred for 30 min, followed by the addition of **16** (34 mg, 0.24 mmol). The stirring was continued for 3 h. The reaction mixture was quenched with saturated NH_4Cl solution and extracted with EtOAc, and the organic layers combined and dried over Na_2SO_4. The solvent was evaporated under reduced pressure and the crude residue was purified by silica gel chromatography using 80% EtOAc/Hex as eluent to afford **17** as a white solid (13.7 mg, 67%). ^{1}H NMR (400 MHz, $CDCl_3$): δ 7.71 (d, *J* = 8.1 Hz, 1H), 7.39 (dd, *J* = 9.3, 7.8 Hz, 1H), 7.18-7.09 (m, 2H), 6.32 (s, 1H), 2.94-2.87 (m, 2H), 2.57 (s, 2H), 2.52 (s, 2H), 1.63 (dt, *J* = 15.2, 7.4 Hz, 2H), 1.39-1.22 (m, 6H), 1.14 (d, *J* = 5.6 Hz, 6H), 0.87-0.79 (m, 3H). ^{13}C NMR ($CDCl_3$): δ 136.76, 135.85, 135.22, 129.38, 124.76, 123.51, 121.09, 120.23, 116.17, 111.43, 37.69, 29.55, 29.47, 29.30, 22.66, 20.06, 14.08.

Synthesis of 1,1-bis(iodomethyl)cyclopropane (19)

To a stirred suspension of Ph_3P (1.53 g, 5.87 mmol) in CH_2Cl_2 (30 ml) was added imidazole (792 mg, 11.64 mmol) at 0 °C followed by I_2 (1.49 g, 5.87 mmol) and the reaction mixture stirred at 0 °C for 30 min. A solution of cyclopropane-1,1-diyldimethanol (**18**) (100 mg, 0.97 mmol) in CH_2Cl_2 (5 ml) was added. The reaction mixture was allowed to warm to rt and stirred for 2 h. The reaction was quenched with brine, extracted with CH_2Cl_2. The combined organic layers were washed with water and then 5% $Na_2S_2O_3$ solution and then was dried over Na_2SO_4. The solvent was evaporated under reduced pressure, and the crude was purified using silica gel chromatography using 1% EtOAc/Hex as eluent to afford **19** (300 mg, 96%). ^{1}H NMR (400 MHz, $CDCl_3$): δ 3.35 (s, 4H), 1.03 (s, 4H).

Synthesis of 2,2'-(cyclopropane-1,1-diyl)diacetonitrile (20)

To a round bottom flask containing KCN (161.8 mg, 2.48 mmol) was added a solution of 1,1-bis(iodomethyl)cyclopropane (**19**) (50 mg, 0.248 mmol) in DMF (2 ml). The reaction mixture was refluxed at 45 °C and stirred for 5 h. Saturated NH_4Cl solution (5 ml) was added and the organic layer was extracted with EtOAc, the combined organic layers were washed with brine, and dried over Na_2SO_4. The solvents were evaporated under reduced pressure and the residue was purified by silica gel chromatography using 30% EtOAc /Hex as eluent to afford **20** (26 mg, 87%). ^{1}H NMR (400 MHz, $CDCl_3$): δ 2.55 (s, 4H), 0.78 (s, 4H).

Synthesis of dimethyl 2,2'-(cyclopropane-1,1-diyl)diacetate (21)

To a round bottom flask containing **20** (45 mg, 0.37 mmol) in methanol (3 ml), was added concentrated sulfuric acid (1.3 ml) dropwise at rt and the reaction mixture was then refluxed at 60-65 °C overnight. The reaction was quenched with cold water and extracted with EtOAc, the combined organic layers were dried over Na_2SO_4 and evaporated under reduced pressure to afford **21** as a colorless liquid (40 mg, 57%). ^{1}H NMR (400 MHz, $CDCl_3$): δ 3.67 (s, 6H), 2.40 (s, 4H), 0.54 (s, 4H).

Synthesis of 2,2'-(cyclopropane-1,1-diyl)diacetic acid (22)

To a stirred solution of **21** (40 mg, 0.21 mmol) in isopropanol (2 ml) was added $LiOH{\cdot}H_2O$ (89 mg) in H_2O (0.2 ml) dropwise and stirred at rt for 6 h. The reaction was quenched with saturated NH_4Cl solution, the organic layer was extracted with EtOAc, the combined organic layers were washed with brine, dried over Na_2SO_4, and the solvents were evaporated under reduced pressure to afford **22** (26.5 mg, 78%). ^{1}H NMR (400 MHz, $CDCl_3$): δ 2.39 (s, 4H), 0.64 (s, 4H). ^{13}C NMR ($CDCl_3$): δ 178.81, 41.76, 14.25, 12.50.

Synthesis of 6-oxaspiro[2.5]octane-5,7-dione (24)

To a round bottom flask containing **22** (150 mg, 0.95 mmol) was added acetic anhydride (23) (5 ml) and refluxed at 130 °C for 6 h. The reaction mixture was gradually cooled to rt and then excess acetic anhydride was evaporated under vacuum to obtain a crude product which was purified by silica gel chromatography using 50% EtOAc/Hex as eluent to afford **24** (93 mg, 70%). ^{1}H NMR (400 MHz, $CDCl_3$): δ 2.63 (s, 4H), 0.64 (s, 4H). ^{13}C NMR ($CDCl_3$): δ 166.05, 39.07, 11.25, 10.63.

Synthesis of 2-(1-(2-(2-hexyl-1*H*-indol-1-yl)-2-oxoethyl)cyclopropyl)acetic acid (25)

To a solution of '**6** (n = 3)' (15 mg, 0.08 mmol) in DMSO was added KOH (22.3 mg, 0.40 mmol) at rt and stirred for 30 min followed by the addition of **24** (20 mg, 0.14 mmol). The reaction mixture was stirred for 3 h. The reaction was quenched by adding saturated NH_4Cl solution, the organic layer was extracted with EtOAc, and the combined organic layers were washed with brine and dried over Na_2SO_4. The solvents were evaporated under reduced pressure, and the crude was purified by silica gel chromatography (50% EtOAc/Hex) to afford **25** (14.5 mg, 57%). HRMS (ESI) *m/z* cald for $[C_{21}H_{27}NO_3 + H]^+$: 342.2064, found 342.2008. ^{1}H NMR (400 MHz, $CDCl_3$): δ 7.70 (d, J = 7.7 Hz, 1H), 7.39 (d, J = 7.0 Hz, 1H), 7.13 (ddd, J = 11.7, 6.7, 4.7 Hz, 2H), 6.33 (s, 1H), 3.13 (s, 2H), 2.93 (t, J = 7.5 Hz, 2H), 2.56

(s, 2H), 1.69-1.55 (m, 2H), 1.29 (dd, *J* = 34.0, 4.6 Hz, 6H), 0.82 (dd, *J* = 6, 5.4 Hz, 3H), 0.67-0.50 (m, 4H). ^{13}C NMR ($CDCl_3$): δ 177.28, 171.48, 142.10, 134.94, 129.00, 122.32, 121.90, 119.19, 113.86, 107.22, 44.43, 40.05, 30.70, 29.72, 28.09, 27.84, 21.59, 13.31, 13.06, 11.53, 11.43.

Synthesis of 5-(2-hexyl-1*H*-indol-1-yl)-3-methyl-5-oxopentanoic acid (27)

To a solution of '**6**, n = 3' (20 mg, 0.10 mmol) in THF (1 ml) stirring at 0 °C was added EtMgBr (1 M in THF, 0.20 ml, 0.20 mmol) and **26** (26 mg, 0.20 mmol, dissolved in 1 ml THF). After stirring at 0 °C for 15 min, the reaction mixture was warmed to rt and stirred for 1.5 h. The reaction mixture was quenched with saturated NH_4Cl solution and extracted with EtOAc, and the organic layers combined and dried over Na_2SO_4. The solvent was evaporated under reduced pressure, and the crude residue was purified by silica gel chromatography to afford **27** (23 mg, 75%) HRMS (ESI) *m/z* cald for $[C_{20}H_{27}NO_3 + H]^+$: 330.2064, found 330.1963. ^{1}H NMR (400 MHz, $CDCl_3$): δ 7.70 (d, *J* = 7.9 Hz, 1H), 7.42-7.33 (m, 1H), 7.19-7.06 (m, 2H), 6.32 (s, 1H), 2.98 (m, *J* = 15.1, 6.6 Hz, 4H), 2.70 (dd, *J* = 13.3, 6.6 Hz, 1H), 2.42 (ddd, *J* = 22.8, 15.6, 6.7 Hz, 2H), 1.69-1.54 (m, 2H), 1.42-1.13 (m, 6H), 1.07 (d, *J* = 6.7 Hz, 3H), 0.81 (dd, *J* = 9.5, 4.4 Hz, 3H).^{13}C NMR ($CDCl_3$): δ 178.16, 172.31, 143.02, 136.01, 130.03, 123.35, 122.89, 120.22, 114.72, 108.16, 45.18, 40.53, 31.71, 30.59, 29.12, 28.93, 27.26, 22.60, 20.04, 14.05.

Synthesis of 4-(2-Hexyl-indol-1-yl)-4-oxo-butyric acid (29)

To a stirred solution of '**6**, n = 3' (39 mg, 0.194 mmol) in DMSO (0.4 ml) was added KOH (54 mg, 0.964 mmol) at rt and stirred for 1 h. Dihydro-furan-2,5-dione (**28**) (58.0 mg, 0.582 mmol) in DMSO (0.3 ml) was added to the reaction mixture and stirred for 2 h. The mixture was quenched with saturated NH_4Cl solution, extracted in EtOAc, dried over Na_2SO_4. The solvents were evaporated and the crude was purified using column chromatography (50% EtOAC in hexane) to afford **29** (5.5 mg, 10%). HRMS (ESI) *m/z* cald for $[C_{18}H_{23}NO_3 + H]^+$: 302.1751, found 302.1691. ^{1}H NMR (400 MHz, $CDCl_3$): δ 7.78 (d, *J* = 7.7 Hz, 1H), 7.41 (d, *J* = 7.6 Hz, 1H), 7.22-7.10 (m, 2H), 6.35 (s, 1H), 3.28 (t, *J* = 6.4 Hz, 2H), 2.93 (t, *J* = 7.5 Hz, 2H), 2.85 (t, *J* = 6.3 Hz, 2H), 1.70-1.55 (m, 2H), 1.30-1.11 (m, 6H), 0.83 (d, *J* = 6.2 Hz, 3H). ^{13}C NMR ($CDCl_3$): δ 176.99, 171.75, 143.19, 136.10, 130.16, 123.51, 123.09, 120.26, 114.90, 108.49, 34.01, 31.69, 30.71, 29.12, 28.96, 28.75, 22.59, 14.04.

Synthesis of 34, 35, 36, 41, 42, 47

The title compounds were synthesized from the commercial corresponding 1H-indole-2-carboxylic acid as described below for **34**.

Synthesis of 6-chloro-1*H*-indole-2-carbaldehyde (31, R = Cl)

To a stirred solution of '**30,** R= Cl' (20.2 g, 103 mmol) in THF (20 ml) was added $LiAlH_4$ (7.8 g, 205.5 mmol) slowly at 0 °C. Once the addition was complete the reaction mixture was allowed to warm to rt and stirred for 14 h. Saturated NH_4Cl solution was added and the organic layer was extracted with EtOAc. The combined organic layers were washed with brine and dried over Na_2SO_4. The solvents were evaporated under reduced pressure to get the crude product (17.5 g), which was used without any further purification. To a stirred

solution of crude '**31'** (17.5 g) in acetonitrile (20 mL) was added activated MnO_2 (33.47 g, 391 mmol) and stirred at rt for 18 h. The reaction mixture was diluted with EtOAc and filtered through celite and florisil layers. The solvents were evaporated under reduced pressure and the crude was purified using flash column chromatography (10% EtOAc/Hex) to afford '**31**' as a brown solid (12 g, 69%). HRMS (ESI) *m/z* calcd for $[C_9H_6ClNO+H]^+$: 180.0216 found 180.0215. ^{1}H NMR (400 MHz, $CDCl_3$): δ 9.77 (1H, s), 9.11 (1H, s), 7.58-7.60 (1H, d), 7.39 (1H, s), 7.18-7.19 (1H, m), 7.07-7.10 (1H, dd). ^{13}C NMR ($CDCl_3$): δ 181.96 (s), 124.41 (s), 122.48 (s), 121.43 (s), 120.66 (s), 114.68 (s), 112.23 (s), 110.88 (s), 100.13 (s).

Synthesis of 6-Chloro-2-hex-1-enyl-1*H*-indole (32, R = Cl)

To a suspension of (1-Pentyl)triphenyl-phosphonium bromide ('**4**, n = 3') (30 g, 72.6 mmol) in THF (40 mL) was added LiHMDS (1.0 M in THF, 65 mL, 65 mmol) at −78 °C atmosphere. The mixture was stirred for 30 min, cooled back to −78 °C, and 6-chloro-1H-indole-2-carbaldehyde (**31**) (5.8 g, 32.3 mmol) in THF (40 ml) was added dropwise. The reaction mixture was allowed to warm to rt and stirred for 3 h. Saturated NH_4Cl solution was added, and the organic layer was extracted with EtOAc. The combined organic layers were washed with brine, dried over Na_2SO_4 and the solvents were evaporated under reduced pressure. The crude was purified by silica gel chromatography (15% EtOAc/Hexane) to afford **32** as a pale yellow solid (6.4 g, 85.0%). HRMS (ESI) *m/z* calcd for $[C_{14}H_{16}ClN+H]^+$: 234.1050, found 234.1050. ^{1}H NMR (400 MHz, $CDCl_3$): δ 8.05 (s, 1H), 7.42 (d, *J* = 8.4 Hz, 1H), 7.37-7.26 (m, 2H), 7.02 (d, *J* = 8.4 Hz, 1H), 6.42-6.31 (m, 2H), 6.11-6.00 (m, 1H), 2.24 (q, *J* = 7.1 Hz, 2H), 1.42 (ddd, *J* = 31.6, 14.9, 7.4 Hz, 4H), 0.93 (t, *J* = 7.2 Hz, 3H). ^{13}C NMR ($CDCl_3$): δ 137.31, 136.76, 130.92, 127.78, 127.56, 121.10, 120.63, 120.41, 110.34, 101.26, 32.67, 31.37, 22.24, 13.94.

Synthesis of 6-Chloro-2-hexyl-1^H-indole (33, R = Cl)

To a stirred solution of '**32**, R = Cl' (1.9 g, 8.13 mmol) in EtOH (20 mL) was added 10% Pd/C (114 mg) under H_2 atm. The reaction mixture was stirred at rt for 6 h and then filtered through celite/florisil. The residue was washed with EtOAc, and the combined filtrate was concentrated under reduced pressure. The crude was purified by flash column chromatography using 10% EtOAc/Hex as an eluent to afford **33** as a brown solid (1.7 g, 89%). HRMS (ESI) *m/z* calcd for $[C_{14}H_{18}ClN+H]^+$: 236.1206, found 236.1224. ^{1}H NMR (400 MHz, $CDCl_3$): δ 7.84 (s, 1H), 7.41 (d, *J* = 8.4 Hz, 1H), 7.26 (s, 2H), 7.03 (d, *J* = 7.9 Hz, 1H), 6.20 (s, 1H), 2.73 (t, *J* = 7.4 Hz, 2H), 2.63 (s, 1H), 1.70 (dd, *J* = 13.9, 6.8 Hz, 2H), 1.35 (d, *J* = 26.4 Hz, 6H), 0.89 (s, 3H).

Synthesis of 5-(6-Chloro-2-hexyl-indol-1-yl)-3-methyl-5-oxo-pentanoic acid (34)

To a stirred solution of '**33**, R = Cl' (1.2 g, 5.09 mmol) in DMSO (10 ml) was added KOH (1.21 g, 21.4 mmol) at rt. The reaction mixture was stirred for 30 min followed by addition of 3-methylglutaric anhydride (**26**) (2.6 g, 21.4 mmol). After 3 h the reaction was quenched with saturated NH_4Cl solution, extracted with EtOAc, the organic layers were combined, washed with brine and dried over Na_2SO_4. The solvents were evaporated under reduced pressure and the crude was purified by silica gel chromatography using 20% EtOAc/Hex as

eluent to afford **34** as a light brown solid (1.285 g, 69.5%). HRMS (ESI) *m/z* calcd for $[C_{20}H_{26}ClNO_3+H]^+$: 364.1679, found 316.1674. ^{1}H NMR (400 MHz, $CDCl_3$): δ 7.90 (s, 1H), 7.35 (d, *J* = 8.2 Hz, 1H), 7.18 (d, *J* = 7.2 Hz, 1H), 6.36 (s, 1H), 3.10 (dd, *J* = 15.6, 5.1 Hz, 1H), 3.00-2.86 (m, 3H), 2.77 (dd, *J* = 13.1, 6.7 Hz, 1H), 2.57 (dd, *J* = 14.6, 4.7 Hz, 1H), 2.41 (dd, *J* = 15.6, 7.2 Hz, 1H), 1.68 (d, *J* = 6.1 Hz, 2H), 1.47-1.37 (m, 2H), 1.37-1.28 (m, 4H), 1.15 (d, *J* = 6.4 Hz, 3H), 0.89 (s, 3H). ^{13}C NMR ($CDCl_3$): δ 177.60, 172.23, 143.14, 136.58, 129.32, 128.28, 123.40, 120.60, 115.31, 107.84, 44.97, 40.47, 31.69, 30.60, 29.18, 28.96, 28.75, 27.27, 22.60, 20.09, 14.07.

5-(6-bromo-2-hexyl-1-H-indol-1-yl)-3-methyl-5-oxo-pentanoic acid (35)

Yield: 41%. HRMS (ESI) *m/z* calcd for $[C_{20}H_{26}BrNO_3+H]^+$: 408.1169, found 408.1078. ^{1}H NMR (400 MHz, $CDCl_3$): δ 8.01 (s, 1H), 7.26 (s, 1H), 7.20 (s, 1H), 6.31 (s, 1H), 3.13-2.80 (m, 4H), 2.70 (dq, *J* = 13.0, 6.5 Hz, 1H), 2.46 (ddd, *J* = 63.5, 15.6, 6.4 Hz, 2H), 1.68-1.57 (m, 2H), 1.42-1.22 (m, 6H), 1.10 (d, *J* = 6.7 Hz, 3H), 0.84 (t, *J* = 7.0 Hz, 3H). ^{13}C NMR ($CDCl_3$): δ 172.15, 143.02, 136.99, 128.62, 126.17, 121.06, 118.09, 117.05, 107.93, 44.93, 31.66, 30.57, 29.10, 28.87, 27.26, 22.58, 20.06, 14.05.

5-(2-hexyl-6-methoxy-1-H-indol-1-yl)-3-methyl-5-oxo-pentanoic acid (36)

Yield: 72%. HRMS (ESI) *m/z* calcd for $[C_{21}H_{29}NO_4+H]^+$: 360.2169, found 360.2152. ^{1}H NMR (400 MHz, $CDCl_3$): δ 7.49 (d, *J* = 1.6 Hz, 1H), 7.33 (d, *J* = 8.5 Hz, 1H), 6.85 (dd, *J* = 8.5, 2.1 Hz, 1H), 6.32 (s, 1H), 3.87 (d, *J* = 7.4 Hz, 3H), 3.17-2.90 (m, 4H), 2.75 (tt, *J* = 13.7, 6.9 Hz, 1H), 2.65-2.33 (m, 2H), 1.68 (dt, *J* = 15.1, 7.5 Hz, 2H), 1.36 (ddd, *J* = 10.9, 10.5, 5.5 Hz, 6H), 1.05 (t, *J* = 6.0 Hz, 3H), 0.89 (t, *J* = 7.0 Hz, 3H). ^{13}C NMR ($CDCl_3$): δ 157.11, 141.19, 137.19, 123.77, 120.30, 110.80, 108.09, 101.06, 77.34, 77.02, 76.70, 55.88, 44.96, 31.72, 30.71, 29.12, 29.03, 27.28, 22.61, 20.08, 14.08.

5-(5-chloro-2-hexyl-1-H-indol-1-yl)-3-methyl-5-oxo-pentanoic acid (41)

Yield: 26%. HRMS (ESI) *m/z* calcd for $[C_{20}H_{26}ClNO_3+H]^+$: 364.1674, found 364.1672. ^{1}H NMR (400 MHz, $CDCl_3$): δ 7.69 (d, *J* = 8.9 Hz, 1H), 7.36 (d, *J* = 2.1 Hz, 1H), 7.11 (dd, *J* = 8.9, 2.1 Hz, 1H), 6.28 (s, 1H), 3.16-2.80 (m, 4H), 2.69 (dq, *J* = 13.4, 6.7 Hz, 1H), 2.55-2.27 (m, 2H), 1.62 (dt, *J* = 15.2, 7.5 Hz, 2H), 1.43-1.13 (m, 6H), 1.08 (d, *J* = 6.7 Hz, 3H), 0.83 (t, *J* = 7.0 Hz, 3H). ^{13}C NMR ($CDCl_3$): δ 176.43, 171.06, 143.14, 133.50, 130.18, 127.53, 122.38, 118.67, 114.81, 106.50, 43.96, 39.21, 30.64, 29.60, 28.08, 27.82, 26.19, 21.57, 19.04, 13.03.

5-(5-bromo-2-hexyl-1-H-indol-1-yl)-3-methyl-5-oxo-pentanoic acid (42)

Yield: 66%. HRMS (ESI) *m/z* calcd for $[C_{20}H_{26}BrNO_3+H]^+$: 408.1169, found 408.1150. ^{1}H NMR (400 MHz, $CDCl_3$): δ 8.01 (s, 1H), 7.26 (m, 2H), 6.31 (s, 1H), 3.13-2.81 (m, 4H), 2.71 (dt, *J* = 13.1, 6.6 Hz, 1H), 2.46 (ddd, *J* = 63.5, 15.6, 6.4 Hz, 2H), 1.70-1.55 (m, 2H), 1.46-1.22 (m, 6H), 1.10 (d, *J* = 6.7 Hz, 3H), 0.84 (t, *J* = 7.0 Hz, 3H). ^{13}C NMR ($CDCl_3$): δ 172.15, 143.02, 136.99, 128.62, 126.17, 121.06, 118.09, 117.05, 107.93, 44.93, 31.66, 30.57, 29.10, 28.87, 27.26, 22.58, 20.06, 14.05.

5-(2-hexyl-3-methyl-1-H-indol-1-yl)-3-methyl-5-oxo-pentanoic acid (47)

Yield: 67%. HRMS (ESI) *m/z* calcd for $[C_{21}H_{29}NO_3+H]^+$: 344.2220, found 344.2191. ^{1}H NMR (400 MHz, $CDCl_3$): δ 7.77-7.71 (m, 1H), 7.48-7.42 (m, 1H), 7.28-7.20 (m, 2H), 3.20-2.94 (m, 4H), 2.79 (dq, *J* = 13.4, 6.7 Hz, 1H), 2.50 (ddd, *J* = 22.8, 15.6, 6.7 Hz, 2H), 2.20 (s, 3H), 1.63-1.52 (m, 2H), 1.43-1.23 (m, 6H), 1.15 (d, *J* = 6.7 Hz, 3H), 0.88 (t, *J* = 6.8 Hz, 3H). ^{13}C NMR ($CDCl_3$): δ 177.66, 171.89, 138.24, 135.13, 131.46, 123.48, 122.63, 118.51, 115.31, 114.51, 45.24, 40.46, 31.69, 29.94, 29.20, 27.28, 27.16, 22.65, 20.07, 14.08, 8.69.

Synthesis of 5-(2-hexyl-1-methyl-1-H-indol-3-yl)-5-oxo-pentanoic acid (48)

To a stirred solution of '**6**, n = 3' (19 mg, 0.09 mmol) in CH_2Cl_2 (1 ml) was added Me_2AlCl (1 M in hexane, 0.189 ml, 0.189 mmol) at rt. After 30 min the anhydride (**7**) (21.5 mg, 0.189 mmol) was added and the reaction mixture stirred at rt for 3 h. The reaction was quenched by adding saturated NH_4Cl solution and extracted with CH_2Cl_2. The combined organic layers were washed with brine and dried over Na_2SO_4. The solvents were evaporated under reduced pressure and the crude was purified using silica gel chromatography (80% Et_2O/ Hexane) to afford **48** (25.3 mg, 92%). HRMS (ESI) *m/z* calcd for $[C_{19}H_{25}NO_3+H]^+$: 316.1907, found 316.1898. ^{1}H NMR (400 MHz, $CDCl_3$): δ 7.97-7.86 (m, 1H), 7.41-7.31 (m, 1H), 7.31-7.20 (m, 2H), 3.74 (s, 3H), 3.17 (dt, *J* = 13.9, 7.4 Hz, 4H), 2.62-2.48 (m, 2H), 2.15 (p, *J* = 7.0 Hz, 2H), 1.70-1.54 (m, 2H), 1.36 (dd, *J* = 31.8, 28.6 Hz, 6H), 0.89 (t, *J* = 6.5 Hz, 3H). ^{13}C NMR ($CDCl_3$): δ 159.79, 178.11, 150.26, 136.74, 125.91, 122.09, 122.00, 120.76, 113.01, 109.76, 41.79, 33.39, 31.64, 29.70, 29.54, 29.43, 29.10, 26.28, 22.63, 19.16, 14.08.

Synthesis of 5-Chloro-2-hexyl-1-methyl-1*H*-indole (49, R = Cl)

To a stirred solution of 5-Chloro-2-hexyl-1H-indole (**33**, R = Cl) (87 mg, 0.368 mmol) in DMSO (3 ml) was added KOH (103 mg, 1.84 mmol) at rt. After 30 min CH_3I (0.12 ml, 1.84 mmol) was added dropwise and the reaction mixture stirred at rt for 3 h. Saturated NH_4Cl solution was added and the reaction mixture extracted with EtOAc. The organic layers were combined, washed with brine and dried over Na_2SO_4. The solvents were evaporated under reduced pressure and the crude was purified using silica gel chromatography (10% EtOAc/ Hexane) to afford **49** (85.4 mg, 92.9%). HRMS (ESI) *m/z* calcd for $[C_{15}H_{20}ClN+H]^+$: 250.1363, found 250.1362. ^{1}H NMR (400 MHz, $CDCl_3$) δ 7.47 (s, 1H), 7.15 (d, *J* = 8.6 Hz, 1H), 7.08 (d, *J* = 8.6 Hz, 1H), 6.18 (s, 1H), 3.63 (s, 3H), 2.7 (t, *J* = 7.52 Hz, 2H), 1.74-1.67 (m, 2H), 1.34-1.33 (m, 6H), 0.90 (t, *J* = 6.76 Hz, 3H). ^{13}C NMR ($CDCl_3$): δ 142.98, 135.74, 128.88, 124.83, 120.57, 119.06, 109.6, 98.36, 31.65, 29.57, 29.11, 28.46, 26.88, 22.60, 14.87.

Synthesis of 5-(2-hexyl-1-methyl-1-H-indol-3-yl)-5-oxo-pentanoic acid (50)

Yield: 92%. HRMS (ESI) *m/z* calcd for $[C_{20}H_{27}NO_3+H]^+$: 330.2064, found 330.1929. ^{1}H NMR (400 MHz, $CDCl_3$): δ 7.85 -7.83 (t, 1H), 7.29 -7.27 (t, 1H), 7.22-7.18 (m, 2 H), 3.68 (s, 3H), 3.14 (t, 2H), 3.05 (t, 2H), 2.49 (t, 2H), 2.16-2.02 (m, 2H), 1.62-1.50 (m, 2H), 1.44-1.35 (m, 2H), 1.32-1.16 (m, 4H), 0.79 (t, 3H). ^{13}C NMR ($CDCl_3$): δ 195.8, 178.1, 150.3, 136.7, 125.9, 122.1, 121.9, 120.8, 113.0, 41.8, 33.4, 31.6, 29.5, 29.4, 29.1, 26.3, 22.6, 19.2, 14.1.

5-(5-chloro-2-hexyl-1-methyl-1-H-indol-3-yl)-5-oxo-pentanoic acid (51)

Yield: 81%. HRMS (ESI) *m/z* calcd for $[C_{20}H_{26}ClNO_3+H]^+$: 364.1674, found 364.1628. ^{1}H NMR (400 MHz, $CDCl_3$): δ 7.93 (s, 1H), 7.29 (d, *J* = 3.9 Hz, 1H), 7.23 (dd, *J* = 8.7, 1.0 Hz, 1H), 3.74 (s, 3H), 3.25-3.15 (m, 2H), 3.09 (t, *J* = 6.9 Hz, 2H), 2.65-2.52 (m, 2H), 2.44 (dt, *J* = 18.1, 7.3 Hz, 1H), 2.16 (p, *J* = 7.1 Hz, 2H), 1.73-1.57 (m, 2H), 1.53-1.31 (m, 6H), 0.92 (t, *J* = 6.7 Hz, 3H). ^{13}C NMR ($CDCl_3$): δ 195.26, 178.70, 151.00, 135.13, 127.95, 126.98, 122.23, 120.46, 112.83, 110.60, 41.63, 33.31, 31.59, 29.63, 29.52, 29.08, 26.39, 22.61, 19.05, 14.06.

Synthesis of 52, 53, 54 and 56

These compounds were synthesized as described for **53**.

Synthesis of 5-(5-Chloro-2-hexyl-1-methyl-1*H*-indol-3-yl)-3-methyl-5-oxo-pentanoic acid (53, R = Cl)

To a stirred solution of '**49**, R = Cl' (85 mg, 0.34 mmol) in CH_2Cl_2 (5 ml) was added Me_2AlCl (1 M in hexane, 1.37 ml, 1.37 mmol) at rt. After 30 min 3-methylglutaric anhydride (**26**) (175 mg, 1.37 mmol) was added and the reaction mixture stirred at rt for 3 h. The reaction was quenched by adding saturated NH_4Cl solution. The organic layer was extracted with CH_2Cl_2 and the combined organic layers were washed with brine and dried over Na_2SO_4. The solvents were evaporated under reduced pressure and the crude was purified using silica gel chromatography (30% Et_2O/Hexane) to afford **51** (106.7 mg, 82.6%). HRMS (ESI) *m/z* calcd for $[C_{21}H_{28}ClNO_3+H]^+$: 378.1836, found 378.1835. ^{1}H NMR (400 MHz, $CDCl_3$) δ 7.90 (s, 1H), 7.26-7.19 (m, 2H), 3.72 (s, 3H), 3.22-3.13 (m, 2H), 3.07-2.92 (m, 2H), 2.79-2.67 (m, 1H), 2.56 (dd, *J* = 15.1, 5.3 Hz, 1H), 2.37 (dd, *J* = 15.0, 7.2 Hz, 1H), 1.68-1.56 (m, 2H), 1.47 (d, *J* = 4.9 Hz, 2H), 1.38-1.28 (m, 4H), 1.15 (d, *J* = 6.6 Hz, 3H), 0.89 (s, 3H). ^{13}C NMR ($CDCl_3$): δ 195.40, 176.62, 151.24, 135.17, 128.05, 126.97, 122.33, 120.44, 113.06, 110.66, 48.99, 40.89, 31.59, 29.68, 29.50, 29.09, 26.57, 26.40, 22.60, 20.51, 14.06.

5-(2-hexyl-1-methyl-1-H-indol-3-yl)-3-methyl-5-oxo-pentanoic acid (52)

Yield: 95%. HRMS (ESI) *m/z* calcd for $[C_{21}H_{29}NO_3+H]^+$: 344.2220, found 378.1702. ^{1}H NMR (400 MHz, $CDCl_3$): δ 7.91-7.85 (m, 1H), 7.36-7.30 (m, 1H), 7.26 (s, 2H), 3.71 (s, 3H), 3.24-3.13 (m, 2H), 3.04 (d, *J* = 6.8 Hz, 2H), 2.83 (dd, *J* = 16.9, 3.2 Hz, 1H), 2.72 (dq, *J* = 13.0, 6.4 Hz, 1H), 2.55 (dd, *J* = 14.9, 5.2 Hz, 1H), 2.34 (ddd, *J* = 31.0, 17.2, 8.0 Hz, 2H), 1.68-1.54 (m, 2H), 1.51-1.27 (m, 6H), 1.12 (t, *J* = 5.1 Hz, 3H), 0.87 (t, *J* = 6.0 Hz, 3H). ^{13}C NMR ($CDCl_3$): δ 195.87, 177.31, 166.22, 150.44, 136.78, 125.91, 122.10, 120.70, 113.30, 109.80, 49.14, 41.12, 37.73, 31.63, 29.50, 29.47, 29.11, 26.68, 26.27, 24.00, 22.61, 20.49, 20.00, 14.06.

5-(5-bromo-2-hexyl-1-methyl-1-H-indol-3-yl)-3-methyl-5-oxo-pentanoic acid (54)

Yield: 54%. HRMS (ESI) *m/z* calcd for $[C_{21}H_{28}BrNO_3+H]^+$: 422.1325, found 422.1157. ^{1}H NMR (400 MHz, $CDCl_3$): δ 7.64 (d, *J* = 8.9 Hz, 1H), 7.52 (d, *J* = 2.0 Hz, 1H), 7.25 (dd, *J* = 8.9, 2.0 Hz, 1H), 6.27 (s, 1H), 3.10-2.81 (m, 4H), 2.69 (dq, *J* = 13.3, 6.6 Hz, 1H), 2.43 (ddd, *J* = 60.4, 15.7, 6.6 Hz, 2H), 1.62 (dt, *J* = 15.2, 7.6 Hz, 2H), 1.42-1.22 (m, 6H), 1.20 (d, *J* =

9.7 Hz, 3H), 1.08 (d, *J* = 6.7 Hz, 3H), 0.82 (dd, *J* = 8.6, 5.2 Hz, 3H). ^{13}C NMR ($CDCl_3$): δ 177.15, 172.12, 144.02, 134.89, 131.70, 126.10, 122.76, 116.23, 107.39, 45.00, 40.18, 31.67, 30.59, 29.71, 29.10, 28.84, 27.21, 22.60, 20.07, 14.07.

5-(6-chloro-2-hexyl-1-methyl-1-H-indol-3-yl)-3-methyl-5-oxo-pentanoic acid (56)

Yield: 68%. HRMS (ESI) *m/z* calcd for $[C_{21}H_{28}ClNO_3+H]^+$: 378.1830, found 378.1702. ^{1}H NMR (400 MHz, $CDCl_3$): δ 7.82 (d, *J* = 8.6 Hz, 1H), 7.31 (d, *J* = 1.8 Hz, 1H), 7.20 (dd, *J* = 8.6, 1.8 Hz, 1H), 3.68 (s, 3H), 3.17 (dd, *J* = 19.2, 11.4 Hz, 2H), 2.99 (ddd, *J* = 40.5, 16.0, 6.9 Hz, 2H), 2.73 (dq, *J* = 13.5, 6.7 Hz, 1H), 2.59-2.28 (m, 2H), 1.67-1.54 (m, 2H), 1.53-1.28 (m, 6H), 1.13 (t, *J* = 6.3 Hz, 3H), 0.89 (t, *J* = 7.0 Hz, 3H). ^{13}C NMR ($CDCl_3$): δ 195.32, 178.31, 150.60, 137.24, 127.99, 124.44, 122.43, 121.65, 113.43, 109.84, 49.16, 41.00, 31.59, 29.59, 29.48, 29.13, 26.46, 26.26, 22.60, 20.35, 14.06.

ACKNOWLEDGMENTS

This work was supported by the Canadian Institutes of Health Research [Grants MOP-6254 and PPP-99490], the American Asthma Foundation [Grant 12-0049], the National Heart, Lung, and Blood Institute [Grant R01HL081873], and the Quebec Heart and Stroke Foundation.

The Meakins-Christie Laboratories-MUHC-RI are supported in part by a Center grant from Le Fond de la Recherche en Santé du Québec as well as by the J. T. Costello Memorial Research Fund. J.R. also wishes to acknowledge the National Science Foundation for the AMX-360 [Grant CHE-90-13145] and Bruker 400 MHz [Grant CHE-03-42251] NMR instruments. The content is solely the responsibility of the authors and does not necessarily represent the official views of the National Heart, Lung, and Blood Institute or the National Institutes of Health.

ABBREVIATIONS USED

5-HEDH	5-hydroxyeicosanoid dehydrogenase
5-HETE	5S-hydroxy-6E,8Z,11Z,14Z-eicosatetraenoic acid
5-HpETE	5S-hydroperoxy-6E,8Z,11Z,14Z-eicosatetraenoic acid
5-LO	5-lipoxygenase
5-oxo-12-HETE	5-oxo-12S-hydroxy-6E,8Z,10E,14Z-eicosatetraenoic acid
5-oxo-ETE	5-oxo-6E,8Z,11Z,14Z-eicosatetraenoic acid
$CDCl_3$	deuterated chloroform
Et_2O	diethyl ether
DMF	dimethylformamide
DMSO	dimethylsulfoxide
EtOAc	ethyl acetate
EtOH	ethanol
fMLP	formyl-met-leu-phe

GM-CSF	granulocyte/macrophage colony stimulating factor
Hex	hexanes
I_2	iodine
IL-8	interleukin 8
iPrOH	isopropanol
KCN	potassium cyanide
KOH	potassium hydroxide
$LiAlH_4$	lithium aluminum hydride
LiHMDS	lithium hexamethyldisilazide
LiOH	lithium hydroxide
LT	leukotriene
MeCN	acetonitrile
MeOH	methanol
MnO_2	manganese dioxide
Na_2SO_4	sodium sulfate
NaI	sodium iodide
NH_4Cl	ammonium chloride
PAF	platelet-activating factor
PPh_3	triphenylphosphine
THF	tetrahydrofuran
TMS	tetramethylsilane

REFERENCES7

1. Haeggstrom JZ, Funk CD. Lipoxygenase and leukotriene pathways: biochemistry, biology, and roles in disease. Chem. Rev. 2011; 111:5866–5898. [PubMed: 21936577]
2. Grant GE, Rokach J, Powell WS. 5-Oxo-ETE and the OXE receptor. Prostaglandins Other Lipid Mediat. 2009
3. Powell WS, Gravelle F, Gravel S. Metabolism of 5(S)-hydroxy-6,8,11,14-eicosatetraenoic acid and other 5(S)-hydroxyeicosanoids by a specific dehydrogenase in human polymorphonuclear leukocytes. J. Biol. Chem. 1992; 267:19233–19241. [PubMed: 1326548]
4. Powell WS, Gravelle F, Gravel S. Phorbol myristate acetate stimulates the formation of 5-oxo-6,8,11,14-eicosatetraenoic acid by human neutrophils by activating NADPH oxidase. J. Biol. Chem. 1994; 269:25373–25380. [PubMed: 7929234]

5. Erlemann KR, Rokach J, Powell WS. Oxidative stress stimulates the synthesis of the eosinophil chemoattractant 5-oxo-6,8,11,14-eicosatetraenoic acid by inflammatory cells. J. Biol. Chem. 2004; 279:40376–40384. [PubMed: 15234979]

6. Graham FD, Erlemann KR, Gravel S, Rokach J, Powell WS. Oxidative stress-induced changes in pyridine nucleotides and chemoattractant 5-lipoxygenase products in aging neutrophils. Free Radic. Biol. Med. 2009; 47:62–71. [PubMed: 19376220]

7. Nakamura M, Shimizu T. Leukotriene receptors. Chem. Rev. 2011; 111:6231–6298. [PubMed: 21526749]

8. Norgauer J, Barbisch M, Czech W, Pareigis J, Schwenk U, Schröder JM. Chemotactic 5-oxo-icosatetraenoic acids activate a unique pattern of neutrophil responses -analysis of phospholipid metabolism, intracellular Ca^{2+} transients, actin reorganization, superoxide-anion production and receptor up-regulation. Eur. J. Biochem. 1996; 236:1003–1009. [PubMed: 8665888]

9. O'Flaherty JT, Taylor JS, Kuroki M. The coupling of 5-oxo-eicosanoid receptors to heterotrimeric G proteins. J. Immunol. 2000; 164:3345–3352. [PubMed: 10706729]

10. Powell WS, MacLeod RJ, Gravel S, Gravelle F, Bhakar A. Metabolism and biologic effects of 5-oxoeicosanoids on human neutrophils. J. Immunol. 1996; 156:336–342. [PubMed: 8598482]

11. Powell WS, Chung D, Gravel S. 5-Oxo-6,8,11,14-eicosatetraenoic acid is a potent stimulator of human eosinophil migration. J. Immunol. 1995; 154:4123–4132. [PubMed: 7706749]

12. Muro S, Hamid Q, Olivenstein R, Taha R, Rokach J, Powell WS. 5-oxo-6,8,11,14-eicosatetraenoic acid induces the infiltration of granulocytes into human skin. J. Allergy Clin. Immunol. 2003; 112:768–774. [PubMed: 14564360]

13. Brink C, Dahlen SE, Drazen J, Evans JF, Hay DW, Rovati GE, Serhan CN, Shimizu T, Yokomizo T. International Union of Pharmacology XLIV. Nomenclature for the oxoeicosanoid receptor. Pharmacol. Rev. 2004; 56:149–157. [PubMed: 15001665]

14. Hosoi T, Koguchi Y, Sugikawa E, Chikada A, Ogawa K, Tsuda N, Suto N, Tsunoda S, Taniguchi T, Ohnuki T. Identification of a novel eicosanoid receptor coupled to $G_{i/o}$. J. Biol. Chem. 2002; 277:31459–31465. [PubMed: 12065583]

15. Jones CE, Holden S, Tenaillon L, Bhatia U, Seuwen K, Tranter P, Turner J, Kettle R, Bouhelal R, Charlton S, Nirmala NR, Jarai G, Finan P. Expression and characterization of a 5-oxo-6E,8Z,11Z,14Z-eicosatetraenoic acid receptor highly expressed on human eosinophils and neutrophils. Mol Pharmacol. 2003; 63:471–477. [PubMed: 12606753]

16. Takeda S, Yamamoto A, Haga T. Identification of a G protein-coupled receptor for 5-oxo-eicosatetraenoic acid. Biomedical Research-Tokyo. 2002; 23:101–108.

17. Iikura M, Suzukawa M, Yamaguchi M, Sekiya T, Komiya A, Yoshimura-Uchiyama C, Nagase H, Matsushima K, Yamamoto K, Hirai K. 5-Lipoxygenase products regulate basophil functions: 5-Oxo-ETE elicits migration, and leukotriene B. (4) induces degranulation. J. Allergy Clin. Immunol. 2005; 116:578–585. [PubMed: 16159627]

18. Sturm GJ, Schuligoi R, Sturm EM, Royer JF, Lang-Loidolt D, Stammberger H, Amann R, Peskar BA, Heinemann A. 5-Oxo-6,8,11,14-eicosatetraenoic acid is a potent chemoattractant for human basophils. J. Allergy Clin. Immunol. 2005; 116:1014–1019. [PubMed: 16275369]

19. Sarveswaran S, Ghosh J. OXER1, a G protein-coupled oxoeicosatetraenoid receptor, mediates the survival-promoting effects of arachidonate 5-lipoxygenase in prostate cancer cells. Cancer Lett. 2013; 336:185–195. [PubMed: 23643940]

20. Grant GE, Rubino S, Gravel S, Wang X, Patel P, Rokach J, Powell WS. Enhanced formation of 5-oxo-6,8,11,14-eicosatetraenoic acid by cancer cells in response to oxidative stress, docosahexaenoic acid and neutrophil-derived 5-hydroxy-6,8,11,14-eicosatetraenoic acid. Carcinogenesis. 2011; 32:822–828. [PubMed: 21393477]

21. Powell WS, Rokach J. Biochemistry, biology and chemistry of the 5-lipoxygenase product 5-oxo-ETE. Prog. Lipid Res. 2005; 44:154–183. [PubMed: 15893379]

22. O'Flaherty JT, Cordes JF, Lee SL, Samuel M, Thomas MJ. Chemical and biological characterization of oxo-eicosatetraenoic acids. Biochim. Biophys. Acta. 1994; 1201:505–515. [PubMed: 7803484]

23. Patel P, Cossette C, Anumolu JR, Gravel S, Lesimple A, Mamer OA, Rokach J, Powell WS. Structural requirements for activation of the 5-oxo-6E,8Z, 11Z,14Z-eicosatetraenoic acid (5-oxo-

ETE) receptor: identification of a mead acid metabolite with potent agonist activity. J. Pharmacol. Exp. Ther. 2008; 325:698–707. [PubMed: 18292294]

24. Powell WS, Gravel S, Khanapure SP, Rokach J. Biological inactivation of 5-oxo-6,8,11,14-eicosatetraenoic acid by human platelets. Blood. 1999; 93:1086–1096. [PubMed: 9920859]
25. Blättermann S, Peters L, Ottersbach PA, Bock A, Konya V, Weaver CD, Gonzalez A, Schroder R, Tyagi R, Luschnig P, Gab J, Hennen S, Ulven T, Pardo L, Mohr K, Gutschow M, Heinemann A, Kostenis E. A biased ligand for OXE-R uncouples Gα and Gβγ signaling within a heterotrimer. Nat. Chem. Biol. 2012; 8:631–638. [PubMed: 22634634]
26. Gore V, Patel P, Chang CT, Sivendran S, Kang N, Ouedraogo YP, Gravel S, Powell WS, Rokach J. 5-Oxo-ETE Receptor Antagonists. J. Med. Chem. 2013; 56:3725–3732. [PubMed: 23581530]
27. Lawson JA, Kim S, Powell WS, FitzGerald GA, Rokach J. Oxidized derivatives of ω-3 fatty acids; Identification of $iPF_{3\alpha}$ -VI in human urine. J. Lipid Res. 2006; 47:2515–2524. [PubMed: 16943517]
28. Huang ZH, Hii CS, Rathjen DA, Poulos A, Murray AW, Ferrante A. N-6 and n-3 polyunsaturated fatty acids stimulate translocation of protein kinase Calpha, -betaI, -betaII and -epsilon and enhance agonist-induced NADPH oxidase in macrophages. Biochem. J. 1997; 325(Pt 2):553–557. [PubMed: 9230140]
29. Serhan CN, Petasis NA. Resolvins and protectins in inflammation resolution. Chem. Rev. 2011; 111:5922–5943. [PubMed: 21766791]
30. Blattermann S, Peters L, Ottersbach PA, Bock A, Konya V, Weaver CD, Gonzalez A, Schroder R, Tyagi R, Luschnig P, Gab J, Hennen S, Ulven T, Pardo L, Mohr K, Gutschow M, Heinemann A, Kostenis E. A biased ligand for OXE-R uncouples Gα and Gβγ signaling within a heterotrimer. Nat. Chem. Biol. 2012; 8:631–638. [PubMed: 22634634]
31. Stamatiou PB, Chan CC, Monneret G, Ethier D, Rokach J, Powell WS. 5-Oxo-6,8,11,14-eicosatetraenoic acid stimulates the release of the eosinophil survival factor granulocyte-macrophage colony stimulating factor from monocytes. J. Biol. Chem. 2004; 279:28159–28164. [PubMed: 15136573]
32. Böyum A. Isolation of mononuclear cells and granulocytes from human blood. Isolation of mononuclear cells by one centrifugation, and of granulocytes by combining centrifugation and sedimentation at 1 g. Scand. J. Clin. Lab. Invest. 1968; 21(Suppl):97–89. 77–89.
33. Howard TH, Oresajo CO. The kinetics of chemotactic peptide-induced change in F-actin content, F-actin distribution, and the shape of neutrophils. J. Cell Biol. 1985; 101:1078–1085. [PubMed: 4040915]
34. Powell WS. Precolumn extraction and reversed-phase high-pressure liquid chromatography of prostaglandins and leukotrienes. Anal. Biochem. 1987; 164:117–131. [PubMed: 2823629]
35. Khanapure SP, Shi XX, Powell WS, Rokach J. Total synthesis of a potent proinflammatory 5-oxo-ETE and its 6,7-dihydro biotransformation product. J. Org. Chem. 1998; 63:337–342.
36. Zamboni R, Rokach J. Simple Efficient Synthesis of LTB_4 and 12-epi-LTB_4. Tetrahedron Lett. 1982; 23:2631–2634.

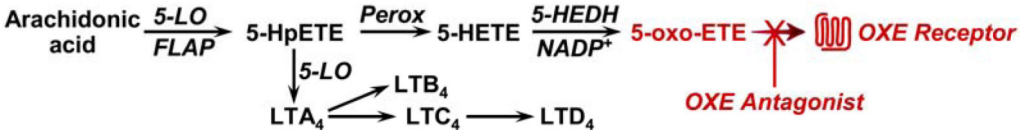

Figure 1.

Biosynthesis of 5-oxo-ETE and its interaction with the OXE receptor. Abbreviation: Perox, peroxidase.

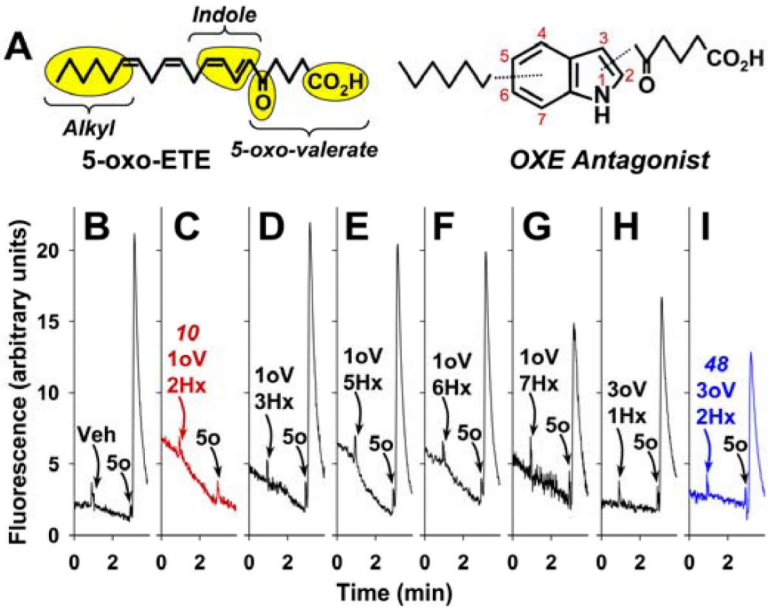

Figure 2. Design and screening of indoles containing hexyl (Hx) and 5-oxovalerate (oV) substituents in different positions

A: Hexyl and 5-oxovalerate groups were placed on an indole scaffold to mimic the corresponding regions of 5-oxo-ETE. Either vehicle (**B**) or indole derivatives containing 5-oxovalerate and hexyl substituents in the 1 and 2 (**C**), 1 and 3 (**D**), 1 and 5 (**E**), 1 and 6 (**F**), 1 and 7 (**G**), 3 and 1 (**H**), or 3 and 2 (**I**) positions, respectively, were added to indo-1 labeled neutrophils as described in the Experimental Section. 5-Oxo-ETE (10 nM) was added 2 min later. One minute later digitonin was added to lyse the cells and release the indo-1 to give the maximal fluorescence response (not shown).

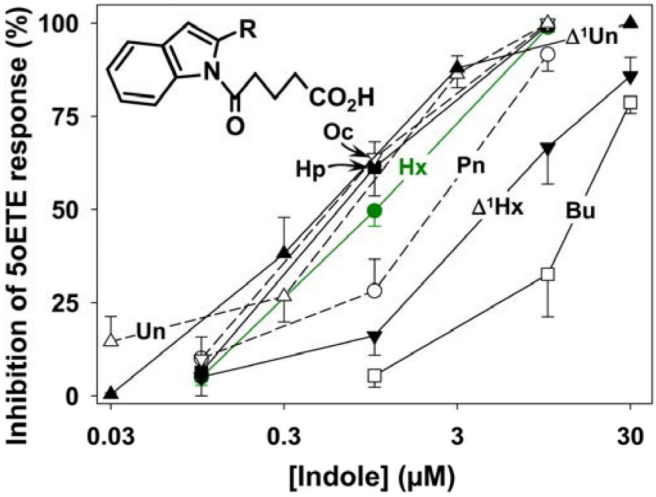

Cpd	Abbr	Smb	R	IC_{50} (μM)
8	Bu	□	butyl	13.7 ± 2.5 (4)
9	Pn	○	pentyl	2.15 ± 0.33 (3)
10	Hx	●	hexyl	1.13 ± 0.16 (13)
14	Δ¹Hx	▼	1-hexenyl	4.03 ± 0.61 (5)
11	Hp	■	heptyl	0.75 ± 0.26 (4)
12	Oc	▽	octyl	0.57 ± 0.10 (4)
13	Un	△	undecyl	0.70 ± 0.10 (6)
15	Δ¹Un	▲	1-undecenyl	0.55 ± 0.29 (5)

Figure 3. Effects of modification of the alkyl group on antagonist potency

The effects of 1-(5-oxovalerate)-indoles containing different alkyl substituents in the 2-position on 5-oxo-ETE-induced calcium mobilization in neutrophils were investigated. Either vehicle or different concentrations of indoles were added to indo-1-loaded neutrophils, followed 2 min later by addition of 5-oxo-ETE (10 nM) as shown in Figure 2. The symbols represent means ± SEM. The IC_{50} values shown in the table to the right are the means ± SE of IC_{50} values from the numbers of independent experiments shown in brackets.

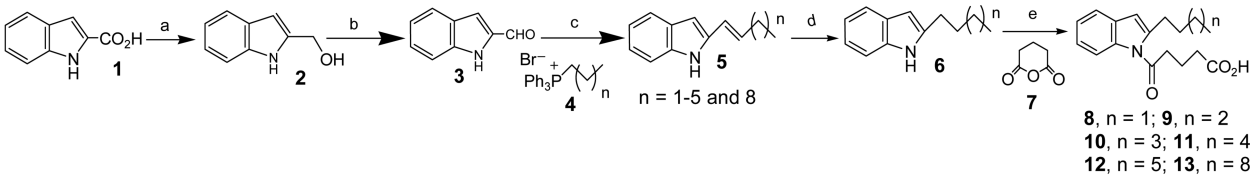

[a]Reagents & Conditions: (a) $LiAlH_4$, THF, 0 °C-rt; (b) MnO_2, CH_3CN, rt; (c) LiHMDS, THF, -78 °C-rt; (d) 10% Pd/C, H_2, EtOH, rt; (e) KOH, DMSO, rt.

Scheme 1.
Synthesis of Alkyl-Substituted 1-(5-Oxovalerate)indoles[a]

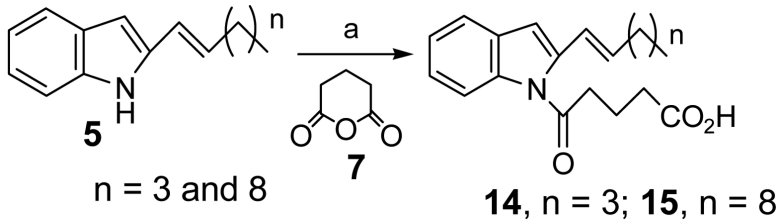

[a]Reagents & Conditions: (a) KOH, DMSO, rt

Scheme 2.
Synthesis of 14 and 15[a]

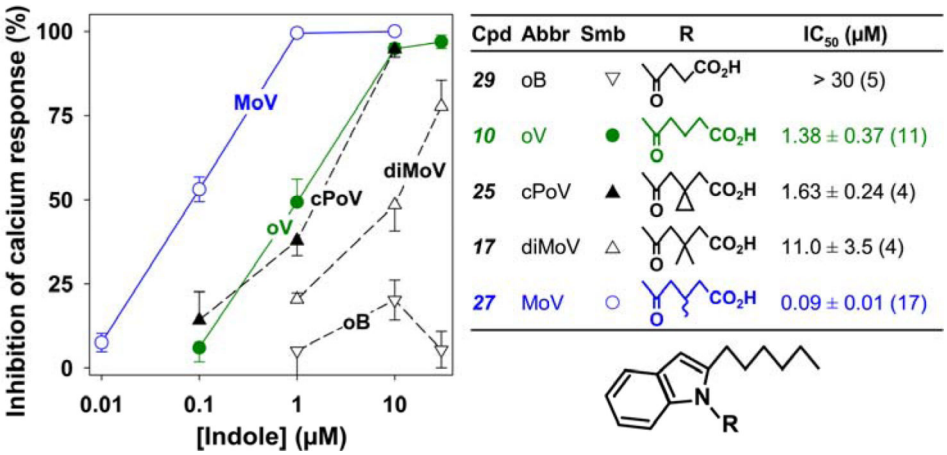

Figure 4. Effects of modification of the carboxyl side chain on the antagonist potency of 2-hexylindoles

Either vehicle or different indoles were added to indo-1-loaded neutrophils, followed by 5-oxo-ETE (10 nM) as shown in Figure 2. The symbols represent means ± SEM. The IC_{50} values were determined as described in Figure 3.

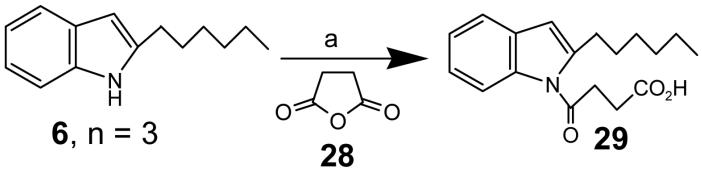

[a]Reagents & Conditions: (a) EtMgBr, THF, 0 °C-rt.

Scheme 3.
Synthesis of 4-(2-Hexyl-indol-1-yl)-4-oxo-butyric acid[a]

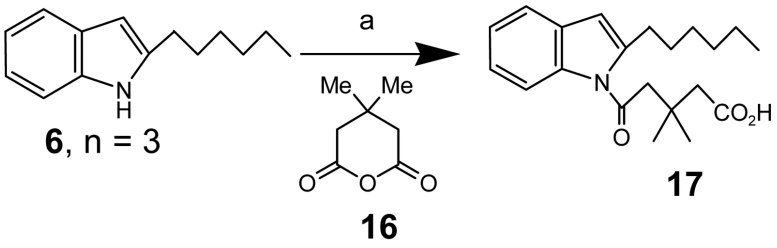

[a]Reagents & Conditions: (a) KOH, DMSO, rt.

Scheme 4.

Synthesis of 5-(2-Hexyl-indol-1-yl)-3,3-dimethyl-5-oxo-pentanoic acid[a]

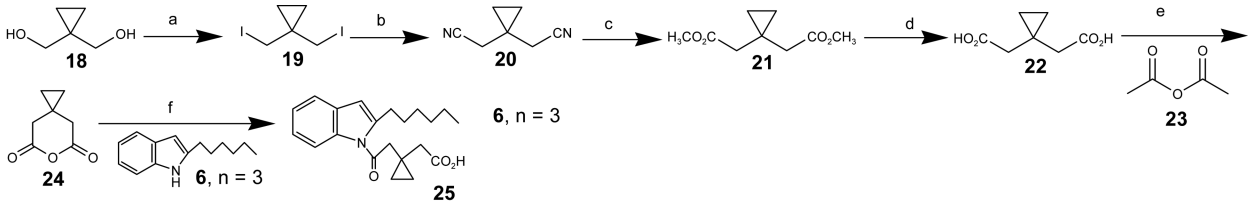

[a]Reagents & Conditions: (a) I_2, PPh_3, Imidazole, rt; (b) KCN, DMF, 45 °C-50 °C; (c) MeOH, H_2SO_4, 60 °C-65 °C; (d) LiOH•H_2O, iPrOH, H_2O, rt; (e) 130 °C (f) KOH, DMSO, rt.

Scheme 5.

Synthesis of 2-(1-(2-(2-hexyl-1H-indol-1-yl)-2-oxoethyl)cyclopropyl)acetic acid[a]

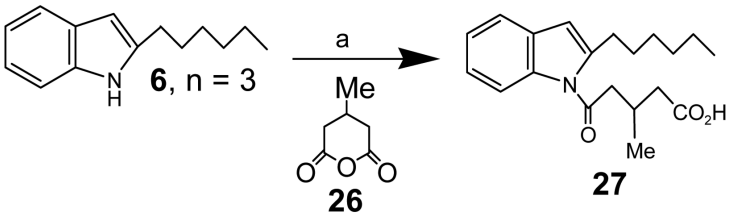

[a]Reagents & Conditions: (a) EtMgBr, THF, 0 °C-rt.

Scheme 6.
Synthesis of 5-(2-Hexyl-indol-1-yl)-3-methyl-5-oxo-pentanoic acid[a]

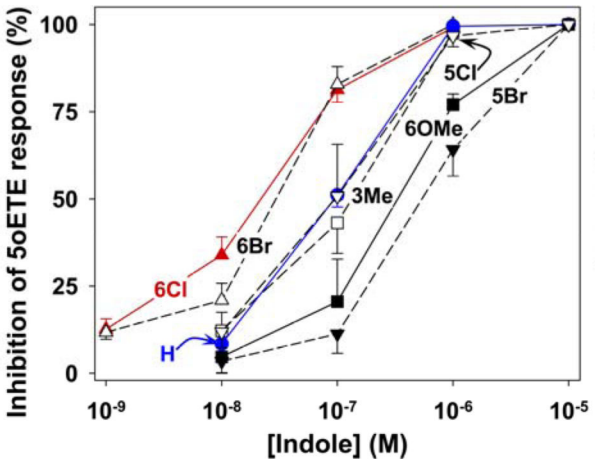

Cpd	Abbr	Smb	R_1	R_2	R_3	IC_{50} (nM)
27	H	●	H	H	H	95 ± 9 (17)
47	3Me	□	Me	H	H	136 ± 45 (4)
42	5Br	▼	H	Br	H	638 ± 164 (4)
41	5Cl	▽	H	Cl	H	141 ± 64 (5)
35	6Br	△	H	H	Br	30 ± 3 (4)
34	6Cl	▲	H	H	Cl	28 ± 5 (16)
36	6OMe	■	H	H	OMe	323 ± 95 (4)

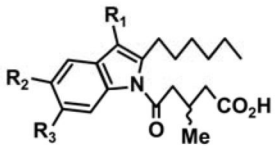

Figure 5. Effects of additional substituents on antagonist potency

The effects of 1-(3-methyl-5-oxovalerate)-2-hexylindoles containing various additional substituents on 5-oxo-ETE-induced calcium mobilization in neutrophils were investigated. Either vehicle or different indoles were added to indo-1-loaded neutrophils, followed by 5-oxo-ETE (10 nM) as shown in Figure 2. The symbols represent means ± SEM. The IC_{50} values were determined as described in Figure 3.

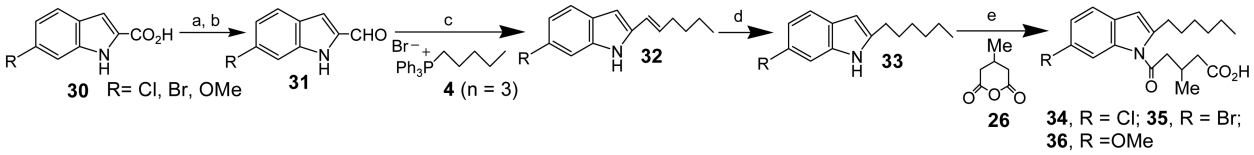

[a]Reagents & Conditions: (a) $LiAlH_4$, THF, 0 °C-rt; (b) MnO_2, CH_3CN, rt; (c) LiHMDS, THF, -78 °C-rt; (d) 10% Pd/C, H_2, EtOH, rt; (e) KOH, DMSO, rt.

Scheme 7.
Synthesis of 34, 35, and 36[a]

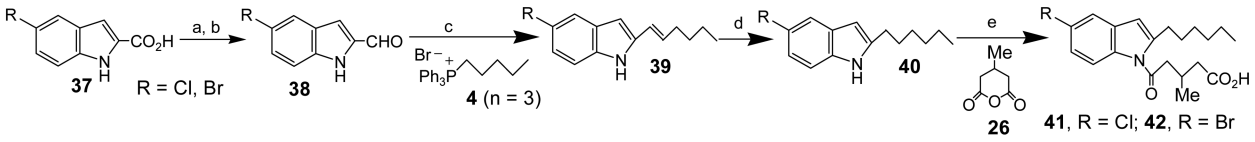

[a]Reagents & Conditions: (a) $LiAlH_4$, THF, 0 °C-rt; (b) MnO_2, CH_3CN, rt; (c) LiHMDS, THF, -78 °C-rt; (d) 10% Pd/C, H_2, EtOH, rt; (e) KOH, DMSO, rt.

Scheme 8.
Synthesis of 41 and 42[a]

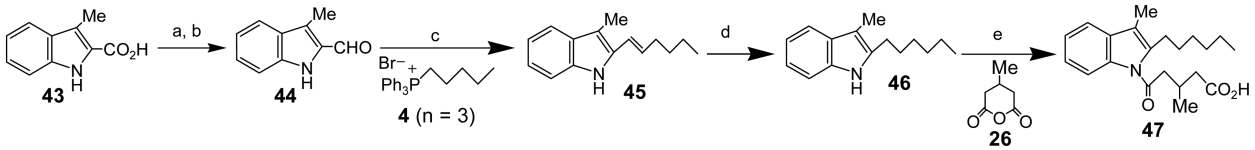

[a]Reagents & Conditions: (a) $LiAlH_4$, THF, 0 °C-rt; (b) MnO_2, CH_3CN, rt; (c) LiHMDS, THF, -78 °C-rt; (d) 10% Pd/C, H_2, EtOH, rt; (e) KOH, DMSO, rt.

Scheme 9.

Synthesis of 5-(2-Hexyl-3-methyl-indol-1-yl)-3-methyl-5-oxo-pentanoic acid (47)[a]

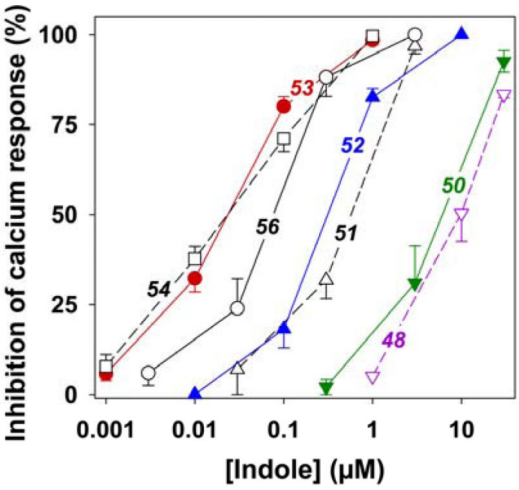

Cpd	Smb	R_1	R_2	R_3	R_4	IC_{50} (nM)
48	▽	H	H	H	H	9,750 ± 2,300 (4)
50	▼	Me	H	H	H	6,060 ± 1,900 (6)
51	△	Me	H	Cl	H	566 ± 92 (5)
52	▲	Me	Me	H	H	314 ± 37 (7)
56	○	Me	Me	H	Cl	81 ± 19 (5)
53	●	Me	Me	Cl	H	28 ± 5 (25)
54	□	Me	Me	Br	H	26 ± 5 (6)

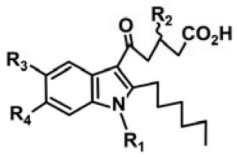

Figure 6. Inhibition of 5-oxo-ETE-induced calcium mobilization by 2-hexyl-3-(5-oxovalerate)-indoles

Either vehicle or different concentrations of indoles, followed by 5-oxo-ETE, were added as shown in Figure 2. The symbols represent means ± SEM. The IC_{50} values were determined as described in Figure 3.

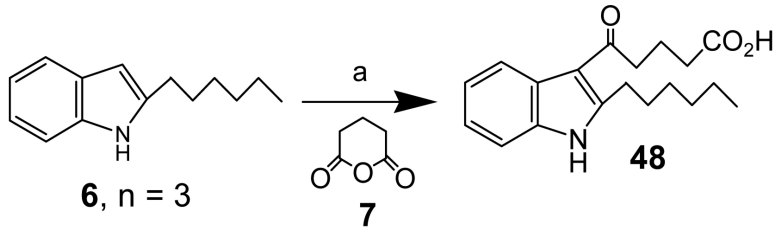

[a]Reagents & Conditions: (a) Me_2AlCl, CH_2Cl_2, rt.

Scheme 10.
Synthesis of 5-(2-Hexyl-1H-indol-3-yl)-5-oxo-pentanoic acid (48)[a]

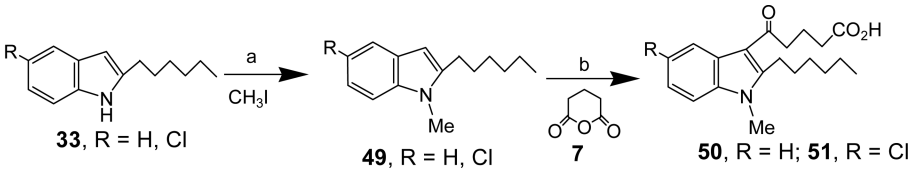

Reagents & Conditions: (i) KOH, DMSO, 0 °C-rt; (ii) Me_2AlCl, CH_2Cl_2, rt.

Scheme 11.
Synthesis of 50 and 51

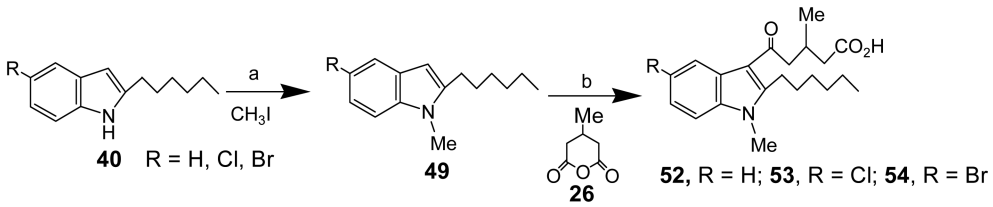

Reagents & Conditions: (i) KOH, DMSO, 0 °C-rt; (ii) Me_2AlCl, CH_2Cl_2, rt.

Scheme 12.
Synthesis of 52, 53, and 54

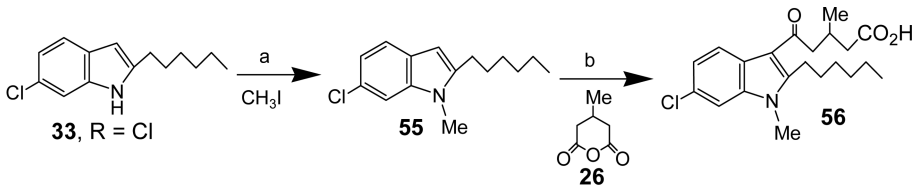

Reagents & Conditions: (i) KOH, DMSO, 0 °C-rt; (ii) Me_2AlCl, CH_2Cl_2, rt.

Scheme 13.

Synthesis of 5-(6-Chloro-2-hexyl-1-methyl-1H-indol-3-yl)-3-methyl-5-oxo-pentanoic acid (56)

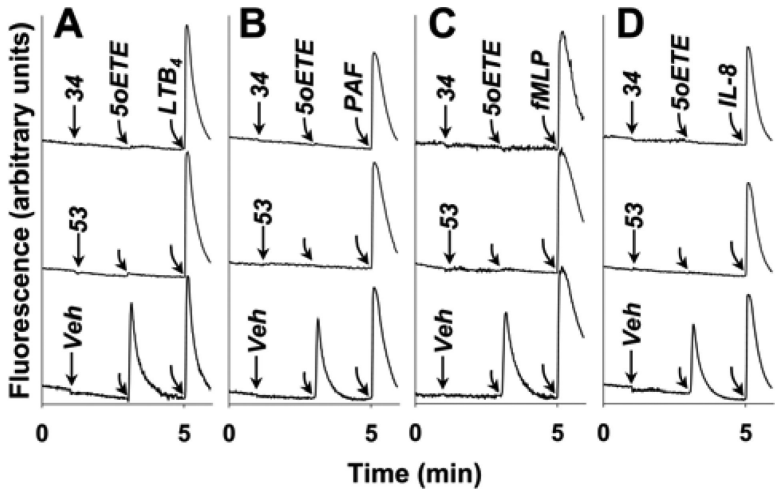

Figure. 7. Selectivity of 53 and 34 for the OXE receptor

The effects of **53** and **34** on calcium mobilization in response to subsequent addition of 5-oxo-ETE followed by either (**A**) LTB_4 (10 nM), (**B**) PAF (10 nM), (**C**) fMLP (100 nM), or (**D**) IL-8 (10 nM). Either vehicle, **53** (10 μM), or **34** (10 μM) were added to indo-1-loaded neutrophils. 5-Oxo-ETE (10 nM) was added 2 min later, followed after a further 2 min by one of the above additional agonists. The results are representative of 2 independent experiments, which had virtually identical results.

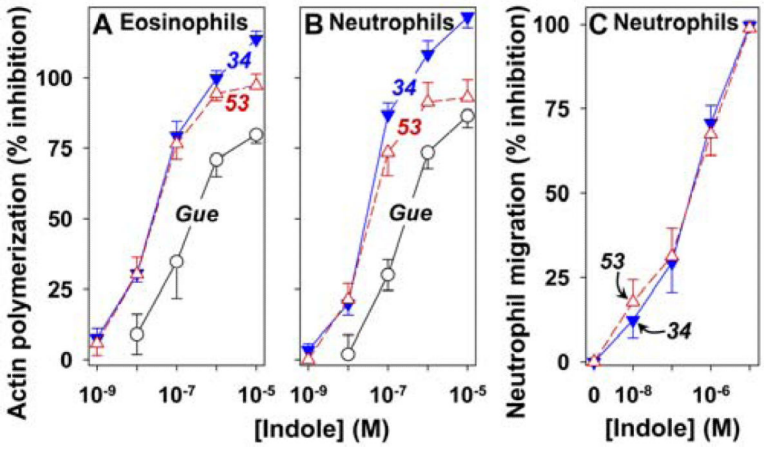

Figure 8. Effects of 53 and 34 on 5-oxo-ETE-induced actin polymerization and chemotaxis

Anti-CD49d-labeled leukocytes were incubated with vehicle, **53** (△; n = 7), **34** (▼; n = 7), or Gue1654 (○; n = 3) for 5 min. 5-Oxo-ETE (10 nM) was then added and 20 s later the incubations were terminated as described in the Experimental Section. Polymerized F-actin was measured by flow cytometry in eosinophils (**A)** and neutrophils (**B).** Neutrophil migration (**C**) was assessed using modified Boyden chambers as described in the Experimental Section. Neutrophils and 5-oxo-ETE (100 nM) were added to the top and bottom chambers, respectively, whereas either vehicle, **53** (△; n = 6), or **34** (▼; n = 8) were added to both the top and bottom chambers. Cells that had migrated through the filter were counted under a microscope (5 fields/well). All data are means ± SE.

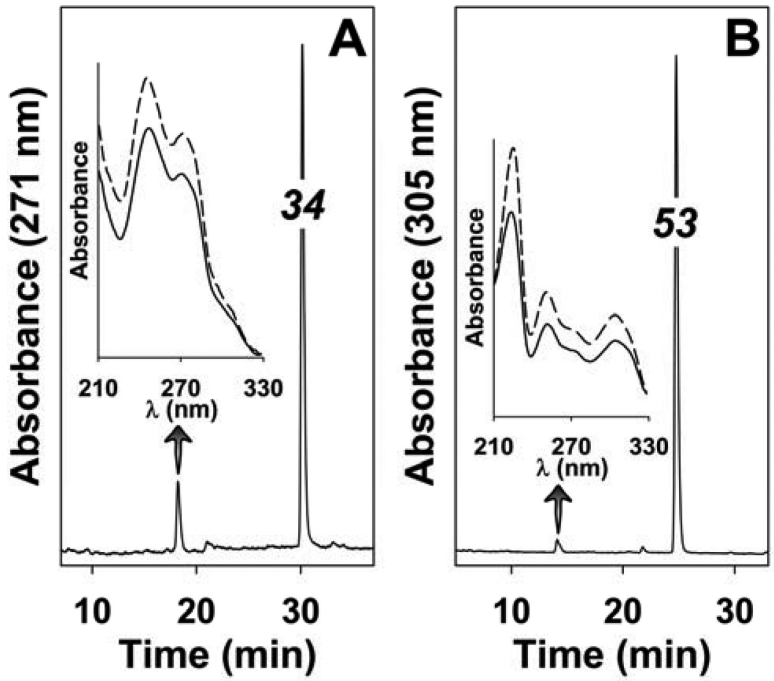

Figure 9. Metabolism of 34 (A) and 53 (B) by rat liver homogenates

Either **34** or **53** (20 μM) were incubated with rat liver homogenates in the presence of NADPH (1 mM) for 60 min at 37 °C and the products analyzed by reversed-phase HPLC as described in the experimental section. The wavelengths monitored were 271 nm (**34**) and 305 nm (**53**). The solid lines in the insets show the UV spectra of the polar metabolites, whereas the broken lines show the spectra of **34** and **53** standards.

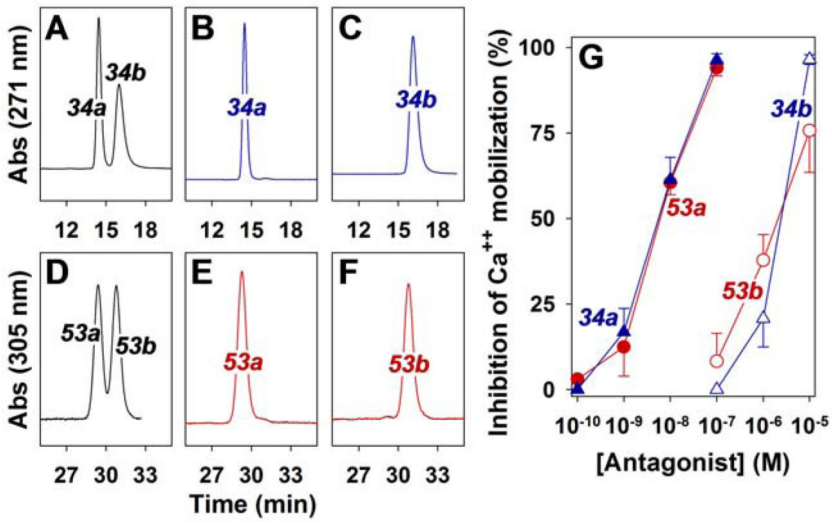

Figure 10. Effects of purified enantiomers of 34 and 53 on 5-oxo-ETE-induced calcium mobilization in neutrophils

Chiral HPLC of **34** on a Lux Amylose-2 column resulted in two peaks (**34a** and **34b; panel A**), which were collected as separate fractions. Analysis of aliquots of the two fractions under identical conditions is shown in panels **B** (**34a**) and **C** (**34b**). Two fractions (**53a** and **53b**) were also obtained after chromatography of **53** on a Lux Cellulose-1 column (**D**). An aliquot from the first peak was analyzed under identical conditions (**E**). The second peak (**53b**) was further purified by a second chromatography to remove a small amount of contaminating **53a** and an aliquot was then analyzed using the same conditions (**F**). The materials in the peaks shown in panels **B** (▲) **C** (△), **E** (●) and **F** (○) were tested for their abilities to block 5-oxo-ETE-induced calcium mobilization in neutrophils (n = 4) as described in the legend to Figure 2 (**G**).

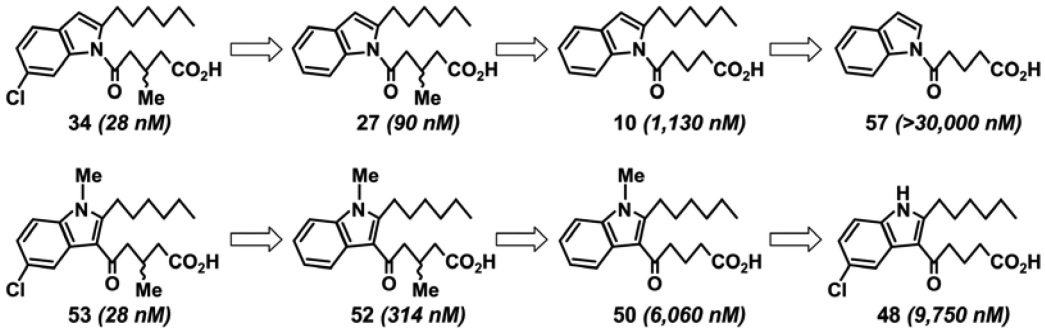

Figure 10.

Summary of the structure-activity relationships leading to the OXE receptor antagonists 34 and 53.